DEPARTMENT OF ONCOLOGY-PATHOLOGY
Karolinska Institutet, Stockholm, Sweden

THE EFFECT OF SPATIAL AND TEMPORAL DOSE DISTRIBUTIONS ON RADIATION-INDUCED SIDE EFFECTS IN THE LUNG

Berit Wennberg

Karolinska Institutet

Stockholm 2011

Published by Karolinska Institutet.

ISBN 978-91-7457-533-0

Printed by
REPROPRINT AB
Stockholm 2011
www.reproprint.se
Gårdsvägen 4, 169 70 Solna

ABSTRACT

In radiotherapy (RT), the aim is to kill all malignant cells in a tumor or to render them incapable of further division and multiplication without producing damage to the normal tissues surrounding the tumor. To achieve this, both the spatial and temporal distribution of dose delivery are important for optimizing the treatment. A sufficiently high dose must be delivered to the tumor cells and as low a dose as possible to normal tissues. The number of fractional doses delivered also impacts outcome due to the time-dependent repair of sublethal radiation damage, which differs in tumor and normal cells. In patients undergoing RT for tumors located in and near the thorax, irradiation of the healthy lung may induce radiation pneumonitis (RP), which can be a serious problem. Understanding the factors involved in the onset of RP is important for reducing its incidence

The overall aim of the thesis was to determine if radiation-induced side effects in lung can be modelled in terms of the spatial and temporal distributions of the doses delivered in conventional RT for breast cancer (BC) and hypofractionated stereotactic body radiotherapy (SBRT) for lung cancer.

Radiological changes in the lung were quantified with Computer Tomography (CT) after RT in 121 patients with breast cancer (BC). Their association with the spatial dose distribution as well as incidence of RP where studied. It was found that RP and radiological findings were associated with the spatial dose distribution. In a subgroup of 87 patients, data of the spatial dose distribution and incidence of RP were modelled using four different normal tissue complication probability (NTCP) models. The studied models fit quite accurately to data for the considered endpoints. Mean lung dose was shown to be a robust and simple parameter that correlated with the risk of RP.

The calculated spatial dose distribution in SBRT of tumors in the lungs, including breathing motions, were assessed for accuracy. The analysis showed that the dose in the central part of the gross tumor volume (GTV) was accurate to within 2–3% for commonly used algorithms; however in the lung tissue close to the GTV the different algorithms both over- and underestimates it, depending on type. When clinically relevant breathing motions were considered, the dose calculated for a static situation remained a relatively accurate estimate of the dose in the GTV. Data of dose distributions and incidence of RP after SBRT for lung cancer were fitted to a NTCP model in a cohort of 57 patients. Correction for fractionation was done in two ways: with the Linear-Quadratic (LQ) model and the Universal Survival Curve (USC). The modelling showed that low dose volumes contributes less to NTCP and high dose volumes comparatively more with the USC model, than the LQ model. The impact of fractionation in SBRT was analyzed using the LQ- and USC models for fractionation correction. The therapeutic window was shown to increase with number of fractions for a range of regimes (2 to 20 fractions) at target doses common in SBRT. Generally, a larger gain was predicted with the USC correction. At high doses per fraction, typical in SBRT, the USC model predicted a lower sensitivity for fractionation as compared to the LQ model.

In conclusion, the incidence of RP can be modelled, accounting for spatial and temporal dose distributions, especially in conventional RT of BC. In SBRT, with a more focused irradiation to very high doses, some uncertainties remain, both regarding the dependence of the spatial dose distribution and particularly of fractionation. The modelling shows that a less extreme hypo fractionation in SBRT may be a way to increase indications for SBRT. Generally, more data is needed for improved modelling.

LIST OF PUBLICATIONS

I. **Wennberg B, Gagliardi G, Sundbom L, Svane G, Lind P**
Early response of lung in breast cancer irradiation: radiologic density changes measured by CT and symptomatic radiation pneumonitis.
Int J Radiat Oncol Biol Phys ***52****(5):1196-206 (2002)*

II. **Rancanti T, Wennberg B, Lind PA, Svane G, Gagliardi G**
Early clinical and radiological pulmonary complications following breast cancer radiation therapy: NTCP fit with four different models
Radiotherapy and Oncology ***82****(3):308-316 (2007)*

III. **Panettieri V, Wennberg B, Gagliardi G, Amor Duch M, Ginjaume M, Lax I**
SBRT of lung tumours: Monte Carlo simulation with PENELOPE of dose distributions including respiratory motion and comparison with different treatment planning systems
Physics in Medicine and Biology ***52****:4265-4281 (2007)*

IV. **Wennberg B, Baumann P, Gagliardi G, Nyman J, Drugge N, Hoyer M, Traberg A, Nilsson K, Morhed E, Ekberg L, Wittgren L , Lund J-Å, Levin N, Sederholm C, Lewensohn R, Lax I**
NTCP modelling of lung toxicity after SBRT comparing the universal survival curve and the linear quadratic model for fractionation correction
Acta Oncologica ***50****(4):518-27 (2011)*

V. **Wennberg B, Lax I**
Analysis of the impact of fractionation in SBRT by the linear quadratic model and the universal survival curve model.
Manuscript

CONTENTS

LIST OF ABBREVIATIONS

3DCRT	3-Dimensional Conformal Radiation Therapy
BC	Breast Cancer
BED	Biologically Effective Dose
CC	Collapsed Cone
CFRT	Conformal Radiotherapy
CT	Computer Tomography
CTV	Clinical Target Volume
DVH	Dose Volume Histogram
EORTC	the European Organization for Research and Treatment of Cancer
EUD	Equivalent Uniform Dose
FEV1	Forced Expiratory Volume in 1 Second
GTV	Gross Tumor Volume
IAEA	International Atomic Energy Agency
ICRU	International Commission on Radiation Units and Measurements
IGRT	Image Guided Radiotherapy
IMN	Internal Mammary Lymph Nodes
IMRT	Intensity Modulated Radiotherapy
LC	Lung Cancer
LET	Ionization Density
LKB	The Lyman-Kutcher-Burman Model
LOGEUD	The Logit-EUD Model
LQ	Linear Quadratic Model
MD	Mean dose
MLD	Mean Lung Dose
MU	Monitor Units
NCI-CTC	The National Cancer Institute Common Toxicity Criteria
NSCLC	Non-Small Cell Lung Cancers
NTCP	Normal Tissue Complication Probability
OAR	Organs at Risk
PB	Pencil Beam Model
PTV	Planning Target Volume
QUANTEC	Quantitative Analysis of Normal Tissue Effects in the Clinic
RP	Radiation Pneumonitis
RS	Relative Seriality Model
RT	Radiotherapy
RTOG	Radiation Therapy Oncology Group
SBRT	Stereotactic Body Radiotherapy
SCLC	Small Cell Lung Cancers
SHMT	Single Hit Multi Target
TCP	Tumor Control Probability
TPS	Treatment Planning System
USC	Universal Survival Curve

1 INTRODUCTION

The aim of radiotherapy[1] (RT) is to kill all the malignant cells[2] in a tumor or to render them incapable of further cell division and multiplication without damage to the normal tissues surrounding the tumor. Owing to the way radiation interacts with matter, avoiding some radiation-induced cell-killing in normal tissue is impossible. However, the differences in radio sensitivity between normal cells and tumor cells, together with minimizing dose to normal tissues facilitates RT without causing excessive damage[1].

In optimizing RT, the following needs to be considered. The accurate determination of the volume in the body that should be treated (containing malignant cells), the accurate determination of the volumes of normal tissues, to which the doses must be restricted in order to avoid side effects[3], the dose that needs to be delivered to the tumor volume as well as the dose restrictions to the normal tissues must be defined. The sequential pattern of dose delivery must also be determined for optimal utilization of the time-dependant repair of radiation damage, which differs in normal cells and tumor cells.

Thus, important considerations for an optimized RT are:

- *The spatial distribution of the dose delivery* with a sufficiently high dose to the tumor cells and sufficiently low dose to normal tissues.
- *The temporal distribution of the dose delivery* to minimize the repair of radiation damage in tumor cells and maximize it in normal cells.

1.1 RESPONSE TO RADIATION IN CELLS

Cells die naturally after maturation followed by senescence. The life time of functional cells varies enormously. The fate of the cells also varies with type of tissue. However, after cytotoxic injury, two types of cell death occurs - interphase death or mitotic death. The latter is the most common and important form of cell death induced by radiation. Since cell death is defined as loss of reproducing capacity (mitotic death) a non-viable damaged cell might appear to be intact even while a locally controlled tumor still is present[4]. When normal tissue is damaged by radiation its regeneration depends on the number of stem cells[5] that have survived and on the integrity of their capacity for proliferation.
An approach to understanding the effect of radiation on tissue involves identifying the target cells and their depletion, effecting tissue function. During the last decades, new insights regarding cells and the cell cycle have increased understanding about how tissues respond to radiation. We know that radiation sensitivity depends of cell type and on their degree of cellular differentiation. Stem cells are the most radiosensitive and fully differentiated cells, which no longer divide, are very radio resistant. The appearance and repair of damage may have different time courses depending on how the tissue are organised. As different tissues have different radio sensitivity and different response to radiation injury

different approaches to RT have to be taken depending on surrounding tissues of the tumor[6].
After irradiation with a very large dose, of several hundred Gray (Gy), all cell function ceases and cell death is immediate. With lower doses of a few Gy to cells that are dividing or that are still able to divide, only a proportion of cells lose their capacity for division or proliferation[4].
The death of clonogenic cells irradiated in-vitro versus the dose given is generally described by an exponential function, i.e. a linear decrease of surviving cells with dose, plotted on a log-linear scale. Accordingly, the clinical experience from RT of macroscopic tumors with a large number of cells is that they require a much higher dose for ablation than microscopic tumors.

The biological factors that influence the response of normal and tumor tissue are summarised by the four Rs of radiotherapy, so-christened by Withers, 1975 [7].
Repair – as seen by cellular recovery during few hours after exposure.
Reassortment – cell cycle progression effect. Cells that survive a first dose of radiation may be in a resistant phase of the cell cycle and then progress into a more radiosensitive phase within a few hours.
Repopulation – during a 4- to 6 week course of RT, tumor cells that survive may proliferate and increase the number of cells that must be killed.
Reoxygenation – in a tumor the resistant hypoxic cells will selectively survive after a dose fraction, but thereafter their oxygen supply increases and their radiosensivity will increase.
Two of these processes will tend to make the tissue more resistant (repair and repopulation) and two more sensitive and as a consequence lately a fifth R has appeared:
Radiosensensitivity- some tumors have a different response to radiation even if allowing for different timing of responses and this is largely due to differences in radiosensitivity.

Models that describe radiation-induced cell kill versus dose are presented below in Chapter 3, *Fractionation effect models*.

1.2 DOSE-RESPONSE CURVES IN TISSUES

The death or damage of cells due to radiation may result in clinical effects, in normal tissues - side effects. Existing descriptions of the mechanisms from cell kill/damage of different cells within an organ, to the final clinical observation of a side effect are largely incomplete[8].
Dose-response curves, i.e. the probability of an observed side effect versus dose, are determined from clinical data of incidence and given dose. A general assumption is that the side effect observed in an organ is directly related to the dose delivered to that organ. This may in some cases not be a complete description, and radiation damage in the vicinity of the organ may be part of the genesis of the observed effect.

Dose response curves are generally assumed to be sigmoid in shape, supported by data[9]. Characteristics of dose response curves are the dose for an incidence of 50% (D_{50}) and the slope of the curve (γ). The D_{50} dose varies markedly between different tissues or organs, depending on the inherent sensitivity and the kinetics of the each type of cells within the organ and the type of response.

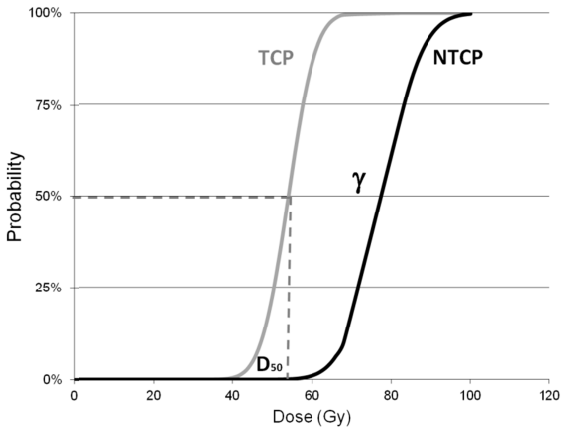

Figure 1. *The therapeutic window – the difference between dose response curves for probability of normal tissue complication (NTCP) vs. tumor control (TCP). Characteristics of dose response curves are shown: the probability of 50% (D_{50}) and the slope of the curve (γ).*

In Figure 1, two dose-response curves are shown. One for the tumor control probability (TCP) and the other for the normal tissue complication probability (NTCP). D_{50} and γ are shown in the figure.

The span in dose between the curves in Figure 1 is called the therapeutic window. The optimal choice of dose is such that it maximizes the TCP and simultaneously minimizes the NTCP. The further a curve for NTCP is displaced to higher doses, (larger therapeutic window) the easier it is to achieve the therapeutic goal. Figure 1 shows an ideal situation. In reality, the TCP curve is often shallower than the NTCP curve, partly because tumors are more heterogeneous than normal tissues. The therapeutic window varies with many factors, primarily on what types of tumor and normal tissues are irradiated. Secondary factors are dose rate, ionization density (LET) of the irradiation, the presence of radio sensitizers or radio protectors, and the design of the treatment plan and the precision of implementing the treatment plan.

Depending on the purpose of the treatment (curative or palliative) the doses to normal tissues may need to be kept lower than the dose to the tumor in order to minimize treatment complications and optimize treatment outcomes. In modern RT, this is achieved through sophisticated 3-D treatment planning (forward or inverse) and dose delivery (conformal or intensity modulated).

Dose-response curves are based on clinical data of incidence of different end-points. Unfortunately, the more severe the end-point, the less accurate data are collected because the incidence is very low[10], resulting in a general lack of data.

1.3 BREAST AND LUNG CANCER

Cancer Incidence

During 2009 there were 54 611 cases of malignant cancers diagnosed and reported to the Swedish Cancer Registry; 53 percent of them in men and 47 per cent in women. The last two decades the average annual increase in number of cases has been 1.9 per cent for men and 1.3 per cent for women. The increase is partly explained by the ageing population but also by the introduction of screening activities and improvements in diagnostic practices[11].

Carcinoma of the Breast

Breast cancer (BC) is the most common malignant tumor in Swedish women representing 29 percent of the female cases in 2009 and today 7000 new cases are diagnosed per year. BC starts in the tissues of the breast and may be invasive, that is spreads from the milk duct or lobule to other tissues in the breast or noninvasive and retain locally in situ.

The treatment for breast carcinoma depends mainly on the tumor's clinical stage when the patient is first seen – surgery and radiotherapy have essential roles as well as hormonal therapies[12-14]. RT is mostly given postoperatively to the afflicted breast or remaining chestwall and depending on tumor stage also to the ipsilateral supraclavicullar, axillary and internal mammary lymph glands (loco-regional). Reactions to RT occur early as well as late but are not often severe. The most common potential late sequelae of RT are chronic changes of the irradiated skin and soft tissue (fibrosis, hyperpigmentation and rarely telangectasias). In patients who undergo axillary node dissection and receive adjuvant irradiation to the axilla, the risk of lymphoedema significantly increases with the addition of radiation. The risk of complications in the joints, ribs (fractures), and brachial plexus is relatively low with current treatment techniques

However, RT for breast cancer has also, until recently, been associated with an increased risk of developing ischaemic heart disease[15]. Furthermore side-effects to the lungs can take the form of acute pneumonitis and sub acute/late lung fibrosis which for some patients can adversely affect the quality of life. When RT is given as an adjuvant treatment and in combination with other treatments such as surgery, hormonal therapy and chemotherapy it is important to minimize RT induced side effects.

Tumors of bronchus and lung

Of all the cancer cases recorded in Sweden during 2009, lung cancer represents 6.3 percent for males and 7 percent for women. Lung cancer is the most common cause of cancer-related deaths in both men and women throughout the world. Lung cancers can arise in any part of the lung, but 90%-95% of cancers of the lung are thought to arise from the epithelial cells, the cells lining the larger and smaller airways (bronchi and bronchioles). Lung cancer tends to spread or metastasize very early after it forms. The lung is also a very common site for metastasis from tumors in other parts of the body.

Pulmonary cancers are broadly classified into two types: small cell lung cancers (SCLC) and non-small cell lung cancers (NSCLC). SCLC comprises about 20%

of all lung cancers and is the most aggressive and rapidly growing of all lung cancers. NSCLC is the most common lung cancer, accounting for about 80% of all lung cancers.
Treatment for lung cancer can involve surgical removal of the cancer, chemotherapy, or RT, as well as combinations thereof[16-18]. The treatment of choice has been radical surgery but only subset of lung cancer patients are suitable candidates for surgery. Common early reactions to RT are lung reactions which range between early transient pneumonitis to more serious late occurring fibrosis, skin reaction and fatigue. For more centrally located lung tumors severe reactions may occur within the esophagus[19].

1.4 ORGANS AT RISK AND DOSE VOLUME CONSTRAINTS

Normal tissues surrounding a tumor may be a dose-limiting consideration in RT by virtue of their near proximity to the target volume (e.g., rectum near the prostate, heart near the left breast, parotids near head and neck tumors) or the tumor's whole or partially localization within a functioning organ (e.g., primary or metastatic tumors or malformations in the liver, lung and brain).
The International Commission on Radiation Units and Measurements (ICRU) provides guidelines for working with radiation. In report 50[20], volumes that must be identified prior to any RT are defined: the gross tumor volume (GTV), the clinical target volume (CTV) and the planning target volume (PTV). Organs at risk (OAR) are defined as normal tissue whose radiation sensitivity may significantly influence treatment planning and/or prescribed dose. Thus a healthy organ may or may not be defined as an OAR, depending on the dose to the organ and volume of the organ to be irradiated.
Dose/volume constraints are available in the litterateur and lists doses that, given to a certain volume fraction of an organ, will cause a specified side effect at a certain level of probability. The latest overview and summary of recommended dose/volume constraints are published by QUANTEC (Quantitative Analysis of Normal Tissue Effects in the Clinic)[21]. The accuracy of dose-response data is limited, as discussed in the QUANTEC report and also below.

1.5 RADIATION INDUCED SIDE-EFFECTS IN LUNG

The principal function of the lungs is to exchange gases between the air we breathe and the blood. The right lung has three lobes, whereas the left lung is divided into two lobes and a small structure called the lingual that is the equivalent of the middle lobe on the right side. The major airways entering the lungs are the bronchi, which arise from the trachea. The bronchi branch into progressively smaller airways called bronchioles that end in tiny sacs known as alveoli, where gas exchange occurs. The lungs and chest wall are covered with a thin layer of tissue called the pleura.
Radiation induced lung injury has two waves of damage. Radiation pneumonitis (RP) occurs after 3 to 6 months and is characterized by interstitial oedema and oedema in airspaces affecting the patient with dry cough, dyspnea and fever. These lesions may be reversible. A later wave of injury occurs after 9 months presumably

results from lung fibrosis. These injuries may increase in severity for up to 1 – 2 years before stabilizing. RT-induced pulmonary complications such as pneumonitis result from injury to type II pneumocytes, and endothelial cells, become manifest after an initial latent period reflecting the inherent turnover time of the affected cells[22]. Late injury from RT appears clinically and histologically as progressive fibrosis, but the mechanism is not completely clear[23].
To diagnose radiation-induced lung injury many different end-points can be used [22, 24]:

- **Radiographic.** Appears within a few months after RT, increases in tissue density associated with acute inflammation or late fibrosis typically seen on either chest x-rays (CXR) or computed tomography (CT). The latter is more sensitive because it provides better 3-dimensional (3D) visualization of the lung [25-27].

- **Clinical.** Acute pneumonitis typically presents 1 to 6 months after RT, with symptoms of shortness of breath, cough and occasionally mild fever. Pneumonitis usually responds well to steroids[22].

- **Late.** Clinically significant RT-induced fibrosis is typically described as progressive chronic dyspnea associated with scarring of the irradiated lung, typically occurring months to years after RT[22, 23].

- **Functional Endpoints**.The primary function of the lungs is to provide oxygen to, and extract carbon dioxide from, the pulmonary circulation. Spirometry assesses the rate of gas movement; the most commonly measured parameter is the forced expiratory volume in one second (FEV1) [28].

Although the ultimate endpoint of "incidence of pulmonary toxicity" differs significantly based on the method used to quantify pulmonary complications, whether it be assessment of patient symptoms, chest radiographs, pulmonary function testing, perfusion studies, or CT scans, studies have suggested that the frequency of pulmonary toxicity can be predicted[29, 30], but RP is a clinically diagnosed factor and, as such, prone to be observer dependent[31]. Work has been done to diagnose RP by objective means with different clinical (lung physiology) and radiological parameters (CT-scan), but correlations to clinically relevant side effects have not yet been established.

Reporting toxicity
As the response of the lungs to radiation is a continuous effect with no clear steps, clear cut definitions of how to score such reaction have to be agreed upon. The National Cancer Institute Common Toxicity Criteria (NCI-CTC) version 2 scale is based on symptoms only (Table 1) [32].

Grade 0	Grade 1	Grade 2	Grade 3	Grade 4
No increase in pulmonary symptoms due to irradiation	Increase in pulmonary symptoms not requiring initiation or increase in steroids and/or oxygen	RT-induced pulmonary symptoms requiring initiation or increase in steroids	RT-induced pulmonary symptoms requiring oxygen	RT-induced pulmonary symptoms requiring intubation or causing death.

Table 1. *The modified National Cancer Institute Common Toxicity Criteria (NCI-CTC) issued by The U.S National Institutes of Health*

The Radiation Therapy Oncology Group/European Organization for Research and Treatment of Cancer (RTOG/EORTC) scoring schema has had extensive use in EORTC and RTOG studies and has been used by other groups as well. This protocol combines clinical symptoms and radiological changes (Table 2) and deals separately with acute and late reactions [33].

Grade 0	Grade 1	Grade 2	Grade 3	Grade 4
ACUTE/				
No change	Mild symptoms of dry cough or dyspnea on exertion	Persistent cough requiring narcotic antitussive agents/ dyspnea with minimal effort but not at rest	Severe cough unresponsive to narcotic antitussive agent or dyspnea at rest/ clinical or radiologic evidence of acute pneumonitis/ intermittent oxygen or steroids may be required	Severe respiratory insufficiency/ continuous oxygen or assisted ventilation
LATE/				
None	Asymptomatic or mild symptoms (dry cough) Slight radiographic appearances	Moderate symptomatic fibrosis or pneumonitis (severe cough) Low grade fever Patchy radiographic appearances	Severe symptomatic fibrosis or pneumonitis Dense radiographic changes	Severe respiratory insufficiency/ continuous O2/ Assisted ventilation

Table 2. *RTOG/EORTC Acute and Late Radiation Morbidity Scoring Criteria for Lungs*

Clinical data using these two different scales have been compared as though they give similar results[34]. The conclusion was that the assessment of radiation-induced

lung toxicity differs depending on the scoring system used. Therefore, caution should be used in comparing results from reports that rely on different scoring scales. A scale based on symptoms only, such as the NCI-CTC scale, may be more appropriate for evaluating long-term toxicity after curative radiotherapy for lung cancer. In presented papers, the NCI-CTC scale is used, with both RP grade 1 and grade 2 (marked) or higher used as end-points.
However, the spectrum of confounding variables can have an impact on normal tissue tolerance. Examples of confounding variables include the use of concurrent chemotherapy, radiation protectors or other biological modifiers, and the interval between radiation courses in patients undergoing a second course of RT. Other related variables include co-morbid conditions (e.g., diabetes and collagen vascular disease), patient age, regional variation of radiosensitivity within an organ, and hierarchal organization of the organ (i.e., whether damage to a portion of the organ affects only that portion or has more widespread effect). Furthermore, an organ may have more than one type of late toxicity that may or may not have different tolerance doses.

1.6 RT FOR BREAST CANCER WITH CONVENTIONAL FRACTIONATION

RT for BC with a curative intent is generally given to halt possible microscopic spread of the tumor in local – (the breast) or loco-regional (breast + regional lymph nodes) volumes after surgical resection of the primary macroscopic tumor. Consequently, the prescribed dose is relatively moderate, on the order of 50 Gy, usually given with 2 Gy per fraction. The factors most closely associated with radiation-induced pulmonary complications of breast cancer treatments are total radiation dose, irradiated lung volume and fractionation schedule. Other factors that also impact the induction of RP are chemotherapy[12] anti-hormonal therapy[35], smoking habits[36] age and lung physiology[37].

The treatment is generally given with a standardized technique and may differ among hospitals, depending on the equipment available. Photon beams of 6 to 15 MV and in some situations electron beams are used. Organs at risk requiring consideration are primarily lungs and on patients with left sided tumor locations also the heart. Although modern-day techniques have significantly reduced the risk of lung and cardiac complications, careful 3-D treatment planning should be used to minimize the radiation doses to these relatively sensitive organs[38]. The dose to the lungs are either high and confined to a relatively small volume fraction as shown in the upper panel in Figure 2, or more smeared out in a higher volume fraction as illustrated in the lower panel.

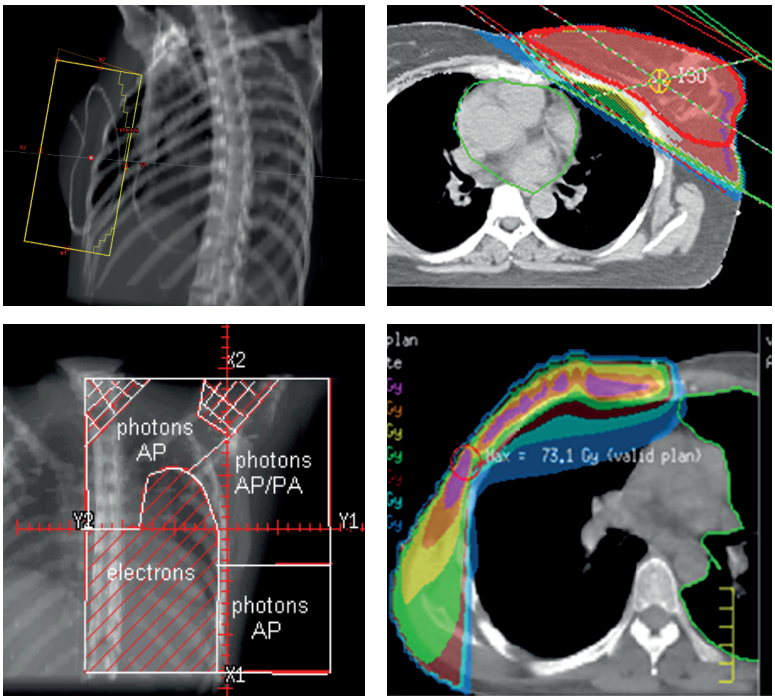

Figure 2 *The upper panels depicts dose distribution of local RT against BC with photons to the breast and the lower panels loco-regional RT for BC as described in 6.1. Dose ranges from low (dark blue) to high (red and cyan).*

QUANTEC recommends that the volume fraction of the lungs that exceeds 20 Gy should be restricted to 30% of the total lung volume in order to yield a probability of symptomatic pneumonitis of less than 20 percent. This recommendation is for a standard fractionation of 1.8 – 2.0 Gy/fraction. QUANTEC also presents a dose-response curve for the same end point. However, as the report states: "The literature on dose/volume parameters and pneumonitis is extensive: for this review we identified > 70 published articles. The results are inconsistent, both for the best predictive metrics and significant comorbid factors"[30].

1.7 STEREOTACTIC RT FOR LUNG TUMORS WITH HYPOFRACTIONATION

SBRT was developed to give ablative doses to solid macroscopic tumors and was pioneered at Karolinska University Hospital twenty years ago[39, 40]. So far this method has been used mainly for solid tumors in the lungs, liver, kidneys and to a minor extent other extracranial locations. As the spatial dose distribution is highly focused to the tumor in SBRT and kept very low to healthy lung, liver or kidney tissues, the temporal dose delivery can be compact, not necessitating the advantage

of very many time gaps for normal tissue repair between each fraction. An SBRT treatment usually consists of 3 to 5 fractions of 15 Gy to 25 Gy/fraction. A short treatment time with hypofractionation as in SBRT has the advantage that repopulation of tumor cells is minimized. As also, hypothesized, the very high dose per fraction could induce apoptosis of endothelial cells and microvascular dysunction in the tumor, which would explain the high control rate of tumors with SBRT[41]. Arguments that used to be raised against a hypofractionation schedule are the probability of increasing late side effects and also decreasing the therapeutic window, due to a reduction in the differential repair of damage of normal- and tumor cells with few fractions. Furthermore, few fractions will reduce the cell kill in the tumors due to reduced reoxygenation and reassortment. Despite the arguments against the way SBRT is delivered, its use has now spread globally because of positive clinical experience[42-46]. In training courses in SBRT at Karolinska University hospital, professionals from about 50 medical institutions worldwide have participated.

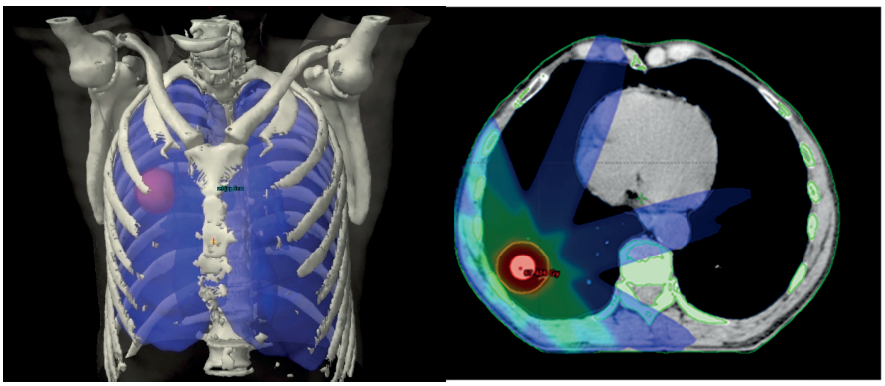

Figure 3. *SBRT in lung cancer, respresenting a highly conformed dosedistribution with a high biological effect.*

Figure 3 illustrates the dose distribution for SBRT of a lung tumor. A steep dose fall-off outside the tumor is obtained with the use of multiple photon beams, on the order of 5-10. The dose to a volume of the lung surrounding the tumor will be very high but due to the steep dose gradient at the periphery of the target the irradiated lung with high dose is very small and consequently the mean dose to the lung will be low. Today, there are usually no dose constraints used for the lung in SBRT of lung tumors. For example, the incidence of symptomatic pneumonitis is on the order of only 10 percent[47].

Comparison of typical lung doses are shown in Figure 4 of conventional fractionated radiotherapy (CFRT) of tumors in the lungs/breast to that of SBRT of tumors in the lungs. The figure shows dose-volume histograms for the lung volume with a relatively large span in spatial dose distribution. Even more pronounced is the span in temporal distribution of the dose delivery with typically 5 to 6 weeks for CFRT as compared to one week for SBRT. An even more extreme case with regard to dose distribution to the lung is the graph representing whole lung irradiation.

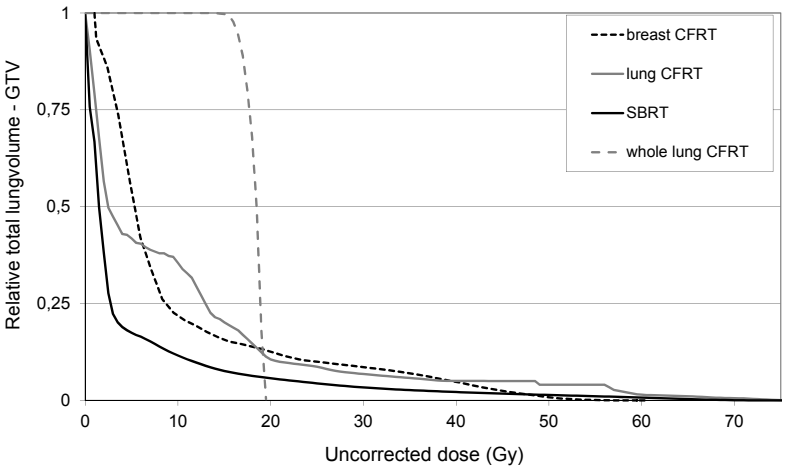

Figure 4. *Representative DVHs for different types of thoracic treatments. Loco-regional BC and lung cancer with CFRT, whole lung irradiation with CFRT and of lung lesions with hypofractionated SBRT.*

In Figure 5, data of the incidence of radiation induced pneumonitis of grade 2 or more (RP2+) is plotted versus mean lung dose (MLD) (from Paper IV). Looking at Figure 5, one is tempted to conclude that MLD is a predictor of lung toxicity separately for RT of the whole lung and for partial lung irradiations such as RT in BC and LC, with different dose-response curves. According to historical data, a MLD of 18 Gy in whole lung irradiation was associated with no toxicity but with conventional treatment techniques (lung cancer and BC) of limited volumes of the lung, the same MLD was instead associated with significant toxicity, up to 15percent (Figure 5). Thus, for the same MLD, the response of the lung depends on the dose-volume characteristic of the irradiation. This observation highlights the question; does a high dose of focused irradiation, as in SBRT, give a different response in the lung compared to that from CFRT? An answer could be that separate volumes of the lungs have different radiosensitivities [48].

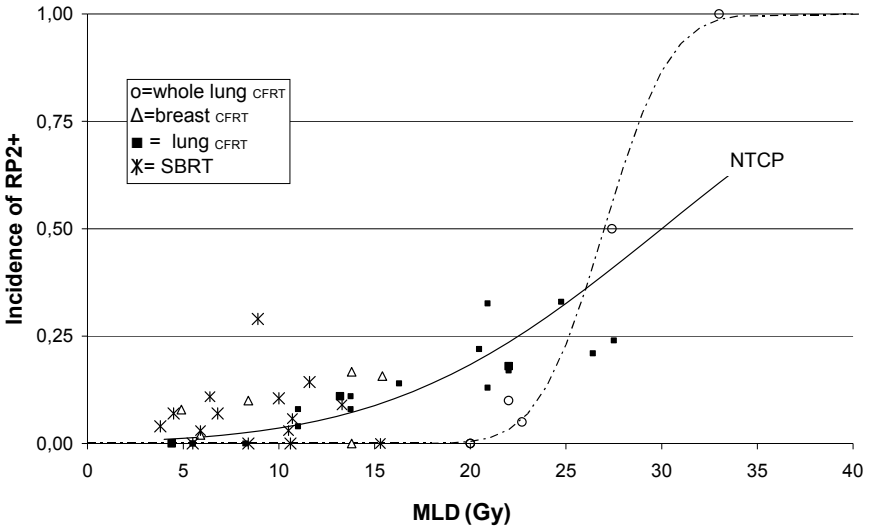

Figure 5. *Incidence of RP2+ as a function of MLD in patients irradiated in the thoracic region. The dashed line is a fit to the data for whole lung irradiation and the solid line a fit to the data for CFRT of breast– and lung cancer.*

The mechanisms of radiation induced lung toxicity are likely to be too complex for a "global" model useful for predicting lung toxicity for all possible techniques used in the clinic.

2 AIM OF THE THESIS

The overall aim of this thesis is to investigate how radiation induced side effects correlates with and can be modelled in terms of the spatial and temporal distributions of the dose delivery in conventional RT for BC and SBRT of lung cancer.

The specific aims of these studies were:

- To quantify radiological changes in the lung with CT after RT for BC and to establish their association with the spatial dose distribution of RT and symptomatic RP. (Paper I)

- To fit data of the spatial dose distribution to the incidence of short-term pulmonary complications in patients treated for BC, using four different NTCP-models. (Paper II)

- To investigate the accuracy of the calculated spatial dose distribution in SBRT of tumors in the lungs, including breathing motions. (Paper III)

- To fit data of the spatial and temporal dose distributions to incidence of pulmonary complications in patients treated with SBRT for lung cancer, using two different models for fractionation correction. (Paper IV)

- To analyze the impact on the probability of pulmonary complications using two different models for fractionation correction in SBRT of tumors in the lungs and study how the therapeutic window is affected by fractionation for a range of regimes of 2 to 20 fractions at target doses common in SBRT. (Paper V)

3 FRACTIONATION EFFECT MODELS

The time period 1920-1930 included an intense debate whether the dose should be given as a single dose to the tumor or divided in several smaller doses, with a time gap in between, for an optimal treatment[4]. Gradually, with increasing clinical experience, it became evident that the therapeutic window could be increased by giving the treatment in many smaller doses. Fractionated RT was thus established. Throughout following decades, several empirical dose-time relations were used for different endpoints. In the 1950ies it became possible to evaluate the proliferative capacity of individual cells, in particular after irradiation. The first survival curves were obtained by in-vitro cloning[49]. A suitable number of cells are seeded in a culture flask. Each cell gives rise to a colony or clone. After irradiation the number of clones is reduced. The surviving fraction is the number of clones surviving after irradiation divided by the number of clones surviving in the absence of radiation. This development gradually established an explanation of dose-time relations in terms of differences in survival curves for different types of cells.

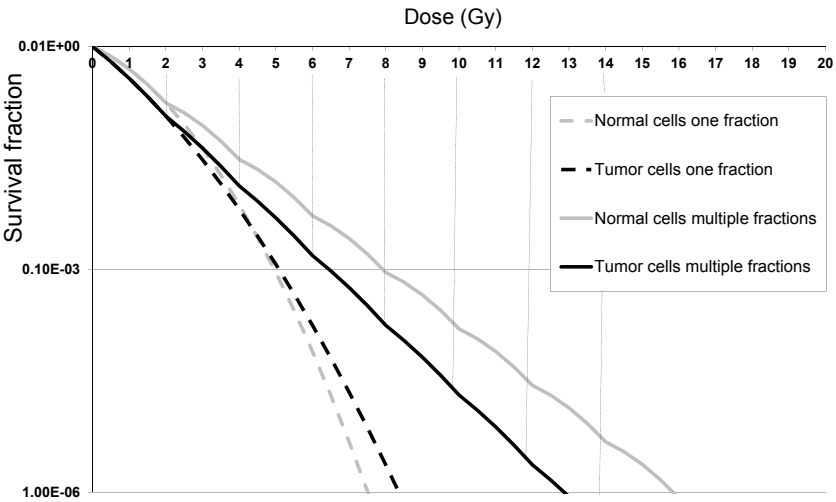

Figure 6. *Survival curves for single radiotherapy doses (dotted lines) to tumor tissue (black) or normal tissue (gray) as well as multiple fractions (solid lines).*

In Figure 6, survival curves for a single fraction given to tumor- and normal cells are schematically shown with dotted lines. The shoulder at low doses represents repair of sublethal damage, with a larger shoulder for the normal cells[4]. The repair process is time dependant. For a time gap of one day between each fraction the repair is generally considered to be complete. Figure 6 also pictures cell survival after fractionated irradiation, assuming complete repair between each fraction and a dose of 2 Gy/fraction (solid lines). The difference in cell death between tumor and normal cells can be considerably increased by fractionation as illustrated in

Figure 6. Two important aspects of fractionation demonstrated here are, first, that the therapeutic window can be increased, and second, that a considerably higher dose must be delivered for the same cell kill with fractionation as compared to that with a single dose.

There are two interpretations of cell survival curves with shoulders.

1. Cell death occurs from an accumulation of events that are individually incapable of killing the cell but together becomes lethal (target model).

2. Lesions are individually reparable but become irreparable and kill cells if the repair mechanism diminish with the number of lesions i.e. dose (repair models).

3.1 EQUIVALENT BIOLOGICAL EFFECT MODELS

Cell survival models can be used to calculate iso-effective doses in fractionated RT assuming complete- or incomplete repair between fractions. To be useful in clinical practice the parameters of the models must be determined from in vivo data. In the following sections some of the target models are described in more detail.

3.2 THE SINGLE HIT MULTI TARGET (SHMT)

The cell is considered to contain $\bar{n}$ distinct and identical targets that are individually affected by radiation. Cell kill occurs when all targets have been inactivated. The surviving fraction of cells after a dose *d* can be described as:

$$S_{SHMT} = 1 - \left(1 - e^{(-d\ /D_0)}\right)^{\bar{n}} \qquad (1)$$

where D_0 and $\bar{n}$ respectively describe the slope and the extrapolation number of the linear part in a plot of the logarithm of survival versus dose. This relationship is based on the hypothesis that damage to the target is random and the probability of a target being undamaged is an exponential function of the dose, $\exp(-d/D_0)$[50]. This model has mainly been used to fit to *in vitro* data.

3.3 THE LINEAR-QUADRATIC (LQ) MODEL

According to this model a cell can be killed in two ways, either by a single-track event or by two-track events and approximates clonogenic survival data with a linear quadratic (LQ) formula[9] where the survival S after a dose of *d* is given by:

$$S_{LQ} = e^{(-(\alpha d + \beta d^2))} \qquad (2)$$

The parameters α and β describes, respectively, the initial slope and the "bending" of the curve in a log-linear plot. After *n* fractions with a dose of *d* per fraction the survival *S* is given by:

$$S_{LQ} = (e^{(-(\alpha d + \beta d^2))})^n \qquad (3)$$

Denoting log of cell kill as the effect of the irradiation E, that is $E = -\ln (S_{LQ})$, equation 3 above can be written:

$$E/\alpha = nd(1 + \frac{d}{\alpha/\beta}) \qquad (4)$$

Fowler suggested that E/α be called the Biologically Effective Dose (BED), which can be described by a single parameter α/β[51]. The significance of the α/β ratio was explained from data collected in fractionation studies in mice[52]. In a log-log plot of iso-effective total dose versus dose per fraction plotted from right to left, there was a systematic tendency that late-responding tissues had steeper iso-effect lines than the early-responding tissues. Thus the sensitivity for fractionation was higher for late responding tissues. Modelling the data with the LQ, later showed that the α/β ratio was lower for late-responding tissues than that for early-responding tissues[4]. From equation 4 it follows that n_1 fractions given with d_1 Gy per fraction gives the same BED as the second fractionation scheme with n_2 fractions given with d_2 Gy per fraction by:

$$n_2 d_2 = n_1 d_1 (1 + \frac{d_1}{\alpha/\beta}) \Big/ (1 + \frac{d_2}{\alpha/\beta}) \qquad (5)$$

The LQ model has been generally accepted both to model *in vitro* data and *in vivo* data and used extensively, especially for low to moderately high doses. However, for a dose per fraction on the order of 15 – 20 Gy as used in SBRT, the LQ model has been questioned[53, 54].

3.4 THE UNIVERSAL SURVIVAL CURVE (USC)

The USC model as suggested by Park was considered to improve descriptions of the cell survival curve especially for very high doses as used in SBRT[54]. In this model, LQ smoothly transitions into the linear part of SHMT (log-lin plot) denoted by linSHMT (equation 6) at the transition dose d_T given by equation 7:

$$S_{linSHMT} = \left(e^{(-d/D_0 + \ln(\bar{n}))}\right)^n \tag{6}$$

$$d_T = \frac{2D_0 \ln(\bar{n})}{1 - \alpha D_0} \tag{7}$$

The USC is represented by equation 3 for doses below the transition dose and by equation 6 for doses above.

$$S_{USC} = \begin{cases} equation\ (3)\ S_{LQ} & if \quad d < d_T \\ equation\ (6)\ S_{linSHMT} & if \quad d \geq d_T \end{cases}$$

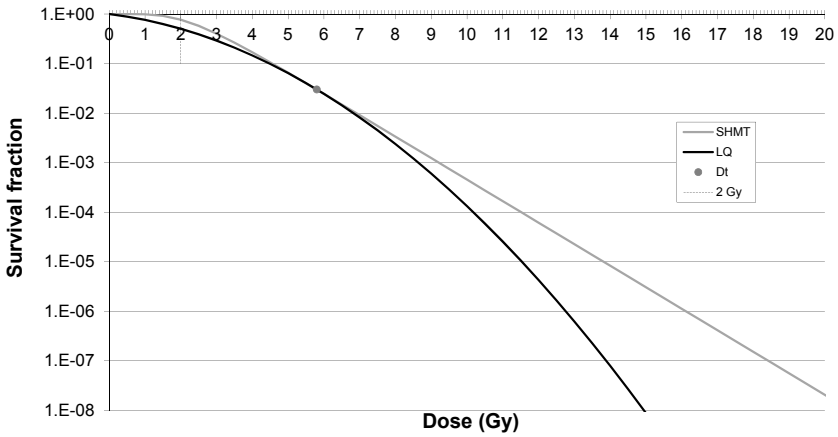

Figure 7. *Survival curves calculated with the LQ model with α/ β=3Gy, and α= 0.206 Gy^{-1} (black line), and with the SHMT model (grey line). The transition from the LQ-model to the linear portion of the SHMT model is at the dose d_T=5.8 Gy (indicated by the circle).*

Figure 7 shows the calculated survival fraction with the LQ and SHMT models. The USC model transforms smoothly from the LQ curve to the SHMT at the point d_T. The USC model has been fitted to *in-vitro* data of cell survival in a more accurate way than the LQ model for survival fractions as low as 10^{-7} [54]. There are four parameters in the USC model but, due to the constraint that LQ smoothly fits into the exponential part of SHMT, it effectively has three parameters[55]. Compared to the two parameters in the LQ model, the USC model has more degrees of freedom in the fitting procedure.

3.5 OTHER MODELS

Other models have been proposed and used to fit to cell survival data. A summary of the ability of different models to fit to cell survival data has been published[55]. A number of different models, including LQ, SHMT and USC, were used to fit to cell survival data for a number of cell lines irradiated to maximum fractional doses of 7 to 15 Gy. More recent models than LQ are now recommended for high fraction doses as used in SBRT[55].

Use of the LQ model has also been suggested for the high dose region with a very high α/β ratio[56] . At an infinitely high α/β ratio, LQ turns into a pure exponential function, similar to the high dose part of the USC model. However, LQ with a very high α/β ratio cannot make correct predictions in the low dose region.

4 EFFECT VERSUS SPATIAL DOSE DISTRIBUTION

Treatment planning and delivery capabilities in radiation therapy have changed dramatically since the introduction of three-dimensional treatment planning systems (TPSs) and are continuing to change relatively rapidly due to the implementation of newer advanced technologies. Three-dimensional conformal radiation therapy (3DCRT) is now firmly in place as the standard of practice in clinics around the world. In intensity modulated radiotherapy (IMRT), the beam fluence is varied optimally to achieve the desired dose distribution that closely conforms to the prescription dose of the target volume and/or avoids specific sensitive normal structures. The increasing use of IMRT, delivered either with static beams or arc therapy, has focused attention on the need to better account for the intra- and inter-fraction spatial uncertainties in the dose delivery process [57].
The continuous technological and methodological developments have improved spatial dose distributions, making possible the delivery of higher doses to target volumes for improved outcomes. Accordingly, the importance and understanding of the relationship between spatial distribution of the delivered dose to OAR and the probability of a specific side effect has become ever more complex.

4.1 HOMOGENEOUS DOSE

Historically, owing to technological limitations, dose distributions conformed less to the target volume and the complete volumes of OAR were relatively often irradiated, and often with a homogeneous dose distribution[58]. In this situation the effect was considered to be a function only of the number of fractions and the dose per fraction as described in Chapter 3. Even today, part of the dose-response data that is available and used in the clinic is based on treatments that was given with a homogeneous dose distribution to the OAR. This applies especially to radiation-induced injuries that appear long after the treatment.
Also for the simplest situation, with a homogeneous dose to the OAR, considerable uncertainties in dose–response curves exist. The causes are due to uncertainties in the actual dose delivered as described later in Chapter 5, but primarily due to difficulties in defining and measuring clinically relevant end-points and the lack of follow-up data consistent with a well defined end-point as discussed in the Introduction.

4.2 INHOMOGENEOUS DOSE

The fact that normal tissues close to the tumor are nearly always non-uniformly irradiated in 3DCRT and especially in IMRT further complicates the use of any model to predict the response of an OAR. With the introduction of 3D dose planning in the beginning of the 1990s, dose-volume histograms (DVH) were also introduced as a way to condense data; however with the loss of the spatial information about the dose distribution within the organ. A DVH gives the percentage of a particular structure that receives a specified dose. They are often graphed as cumulative DVHs, showing the cumulative volume versus dose. Today, DVH data are generally used to correlate with incidence data for the generation of

dose-response curves. From the DVH, dose-volume parameters such as maximum dose (D_{max}), mean dose (MD), equivalent uniform dose (EUD, described below) and dose-volume constraints ($V_{x\ Gy}$) are defined. Yorke presented an overview of methods for modelling the effects of inhomogeneous dose distributions in normal tissues already in 2001 [59].

Regarding RP, several of the DVH parameters have been correlated with incidence data including factors such as $V_{30\ Gy}$, $V_{20\ Gy}$, $V_{13\ Gy}$, and $V_{5\ Gy}$ and MD. $V_{20\ Gy}$ of total lung volume is the most commonly used dosimetric descriptor in practice. It has also been shown that all $V_{x\ Gy}$ are highly correlated with each other[60].

In Figure 8, the different dose-volume parameters are illustrated in a cumulative DVH. To consider fractionation effects in a consistent way, the dose in each bin of the DVH should be corrected to a standardized fractionation with a correction model such as the ones previously described. The lung is usually classified as an organ with a parallel organization of the functional subunits[61]. However, that concept is abstractions of mathematical models and should not primarily be interpreted in anatomical or physiological terms. For these organ types, the mean dose correlate well to incidence data. For other organs described as serially organized, such as the spinal cord, the maximum dose correlate better with the incidence of a side-effect.

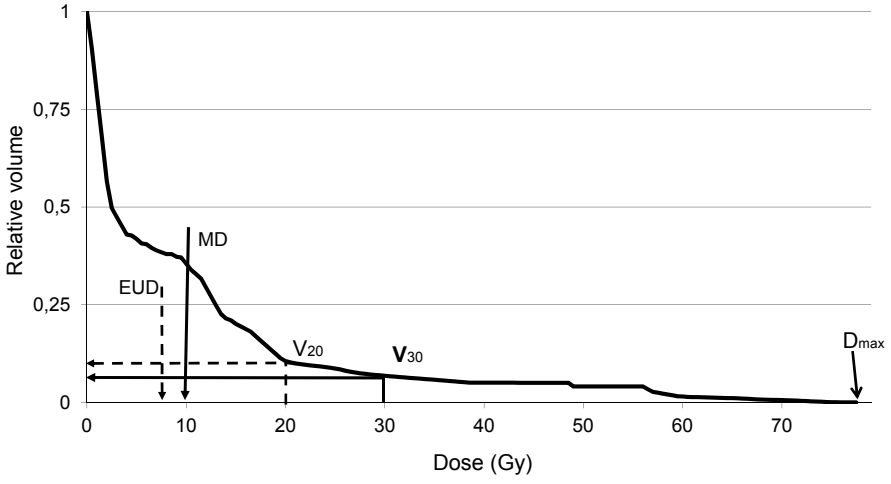

Figure 8 *Depicting DVH with examples of dosimetric predictors V_{20Gy},V_{30Gy},D_{max}, MD and EUD included.*

4.3 NTCP MODELS

Normal Tissue Complication Probability (NTCP) models, although complex, have the attractive feature of considering the complete dose distribution throughout the organ of interest. There are a number of NTCP-models[62], of which many are based on three tissue-specific and endpoint-specific parameters in order to predict the response to radiation. Usually one parameter, describes the dose at which a 50% probability of the response in question is predicted (D_{50}), a second parameter describes the slope of the dose-response curve, and one third describes the volume dependence of the tissue in question.

The Lyman-Kutcher-Burman model, LKB:
This model uses the probit formula to describe the dose-response relationship, characterized by the parameters D_{50} and m (the slope of the response curve at D_{50})[63-65]. When considering non-uniform dose distributions, the differential DVH is converted to an equivalent uniform dose (EUD, equation 9). The parameter n determines the relative importance of different volume fractions. More explicit, *n* is a volume dependence parameter. NTCP is calculated by:

$$NTCP = \frac{1}{\sqrt{2\pi}} \int_{-\infty}^{t} e^{\frac{-x^2}{2}} dx \qquad (8)$$

where

$$EUD = \left(\sum_i D_i^{\frac{1}{n}} \frac{V_i}{V_{tot}} \right)^n \qquad (9)$$

$$t = \frac{EUD - D_{50}}{m \cdot D_{50}} \qquad (10)$$

D_i and V_i are respectively the dose to the corresponding volume of the ith bin of the differential DVH.

The Logit+EUD model, LOGEUD:
This model uses the logit formula coupled with the generalised-EUD reduction algorithm[66] by equation 11. The logit formula describes the dose-response relationship for normal tissues through D_{50} and *k* (the slope of the response curve at D_{50}):

$$EUD = \left(\sum_i v_i D_i^{\frac{1}{n}} \right)^n \qquad (11)$$

$$NTCP(D) = \frac{1}{1 + \left(D_{50} / D \right)^k} \qquad (12)$$

where Di and vi are, respectively, the dose to the corresponding relative volume of the ith bin of the differential DVH.

The Mean-Dose model, MD

This model is derived from the LOGEUD model when the volume effect parameter (n) is equal to one [67]. The DVH is thus reduced to the mean dose (MD) and NTCP is calculated through equation 13:

$$NTCP(MD) = \frac{1}{1+\left(D_{50}/MD\right)^{k}} \qquad [13]$$

The relative seriality model, RS

This model is based on Poisson statistics and it accounts for the architecture of the organ through the parameter of relative seriality s[61]. The relative seriality is derived from the ratio of serial subunits to all subunits in the organ. For a heterogeneous dose distribution the complication probability is given by:

$$NTCP = \left\{1 - \prod_{i=1}^{M}\left[1 - P\left(D_i\right)^{s}\right]^{\Delta v_i}\right\}^{\frac{1}{s}} \qquad [14]$$

where M is the number of calculation subvolumes in the dose calculation volume, D_i is the dose in the subvolume considered and $\Delta v_i = v_i/V$ where v_i is the volume of each subvolume in the DVH and V is the total volume of the organ. P(D) is the Poisson dose-response relationship:

$$P(D) = 2^{-\exp\left(e\gamma\left(1-\frac{D}{D_{50}}\right)\right)} \qquad [15]$$

where D_{50} is the uniform dose that causes 50% probability of injury and γ is the slope of the response curve at D_{37}.

Several NTCP models and many DVH parameters may seemingly accurately describe the risk of RP for broad populations of patients. However, a statistically significant association or description of complication rates for populations of patients may not be the same thing as a good predictor of toxicity for an individual patient due to inherent differences in radiation sensitivity among patients. Many published studies on the incidence of RP are also limited at least in the following aspects: the number of toxicity-events is low with large statistical uncertainties as a consequence; data were mostly from patients treated with RT without the use of 3DCRT, IMRT, stereotactic RT, or proton therapy. The conclusions of the studies might then be appropriate only for the study of specific populations.

5 UNCERTAINTIES IN PATIENT DOSES.

Dose-response data in the literature contain considerable uncertainties[31]. The problems with quantifying responses in the lung are described in Chapter 1.5. This chapter concerns the problem with uncertainties in dose delivered to the patient where geometrical uncertainty is one part and uncertainties in dose calculation, dose delivery and conversion to biological equivalent dose is another part. The goal is to determine the "true dose" delivered to an individual patient over the complete course of the RT, for the generation of accurate dose-response data[68].

Spatial uncertainties

In the RT process, one of the first steps is the definition of target and OAR volumes. Depending on the type of images used in this step, contrast resolution in the images will to a large extent determine the accuracy in the delineation, apart from the skill of the responsible physician. Spatial uncertainties about dose delivery are usually separated into two categories: variations in the positioning of the patient's bony anatomy with respect to the beam (*setup errors),* and variations in the position/shape/size of the target and OAR within the patient with respect to the bony structures (*organ motion/deformation)*. Organ motion can be sizeable as a result of breathing, leading to significant increase in the volume of normal tissue irradiated. Target motions due to breathing may be accounted for both in the CT before dose planning and in the treatment by, respectively, 4D-CT and gating during the treatment.

Multiple strategies are available for increasing the geometric precision of RT, including immobilization and setup aids for reducing random and systematic components of setup errors and organ motion alike. Alternatively, more complex strategies can be implemented based on additional information with the use of image guided radiotherapy (IGRT) acquired over the course during which corrections can be made off-line and on-line[69]. The strategies that are implemented in the clinic must include the required geometric precision for a given treatment, where 3DCRT have larger margins owing to respiratory motions compared to SBRT, during which breathing motion often is reduced by abdominal compression.

Dose uncertainties

Spatial uncertainties, both systematic and random (including breathing motions) will transform into uncertainties about dose. Today attempts are made to develop software in which dose is accumulated throughout the course of the treatment based on imaging during the treatment in order to determine the actual dose delivered[68]. However, this section will deals with uncertainties in dose calculation and in dosimetry for the static situation based on non-4D imaging.

Much of dose-response data available and in clinical use today stems from the time when dose calculations were done with relatively simple pencil beam algorithms[70]. Regarding dose to lung tissue it may even be that correction for the lower density in lung was not performed[71, 72]. As an example of errors caused by simple pencil beam algorithms, we now know that they overestimate the dose to the lung tissues, located close to unit-density tissues[73].

In the simple pencil beam algorithms, correction for tissues that deviate from water is performed only along a straight path, i.e., the pencils, but not laterally. In superposition-convolution algorithms, now in general use in TPS today also the change in lateral transport of secondary particles in non-water media is accounted for. In that method, dose contributions from the primary and scattered radiation are calculated separately. For each point in a volume (voxel), the corresponding attenuation coefficient is determined from the CT data, and the primary radiation beam is attenuated accordingly. A kernel, representing the distribution of scatter from that point, is then applied to each voxel, weighted according to the amount of primary radiation that was attenuated at that point and with the scatter kernel scaled according to the mean density between the points of energy release and deposition. By summing doses from the primary radiation and scattered radiation arising from each voxel, a more accurate dose distribution is generated compared to simple pencil beam algorithms. In benchmarking of dose planning algorithms, Monte Carlo generated data for complex geometries like patient data is often used. Currently, dose planning algorithms based on Monte Carlo simulations are available, and are considered to be the most accurate algorithms, although advanced superposition-convolution algorithms are relatively close.

Uncertainty about the dosimetry, i.e. the calibration of the monitor ion chamber of the treatment unit and/or changes in beam characteristics, such as beam flatness, are judged to be a minor source of error at present. More important is the effect of different fractionations used in the data gathered, for determination of dose-response curves. Unfortunately this is far from always considered[58].

In summary, considerable uncertainty remains about dose data as well as incidence data that was used for determination of some of the dose-response relations in use today[74]. However, one could argue that dose-response data generated by a particular methodology has primarily clinical relevance in the same methodological context. An example would be lung-dose effects after RT of BC, always 2 Gy/fraction to the target volume, the use of a simple pencil beam algorithm for dose planning and no correction for fractionation. But with a view toward the future, this of course, is not creative for generation of improved dose-response data and or for the development of RT. Suggestions and initiatives are taken to pool high-quality datasets from multiple institutions in order to improve the modelling[74].

6 MATERIAL, METHODS AND RESULTS

The effect of spatial and temporal dose distributions on radiation induced side effects in the lung were investigated, for both conventional RT for breast cancer and SBRT for lung cancer.

6.1 CONVENTIONAL RT FOR OF BREAST CANCER (PAPERS I, II)

Four hundred and seventy-five BC patients, referred to the Radiotherapy Department at Stockholm Söder Hospital (1994–1998) for adjuvant post-operative RT were prospectively followed for pulmonary complications 1, 4 and 7 months after the completion of RT. Prescribed doses were 46 Gy or 50 Gy in 2 Gy fractions. The frequencies of RP requiring corticosteriods at Södersjukhuset were found to be 10 % among patients treated with loco-regional RT including the IMN. The results also showed that irradiated lung volume was associated with RP and that the estimated risk increased if more than 30% of the ipsilateral lung volume received more than 20 Gy[75]. A subset of patients who were diagnosed with severe pulmonary complications needing cortisone treatment had a significant functional loss comparable to 15 years of normal ageing or the loss of 3/4 of a lung lobe compared to the patients who were asymptomatic when measured at 6 months after RT[38].

In paper I radiological changes in the lung tissue after RT for BC were quantified with CT in 121 of the patients included above. The association of radiological changes with spatial dose distribution and symptomatic RP was documented. CT scans were performed at two levels through the lungs before RT and 4 months afterwards, one at a level of about 3 cm above the mamillary plane and one at an apical CT slice at the superior aspect of the clavicular head as shown in Figure 9. The change in mean density (Hounsfield number) was measured in three different regions (entire slice, anterior half and anterior third) for each of the two levels. In Figure 10 typical density change after RT for loco-regional RT is shown.

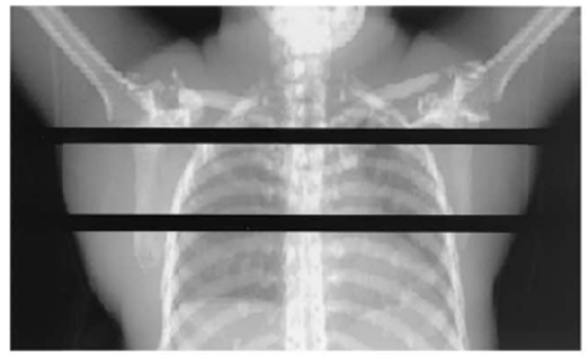

(A)

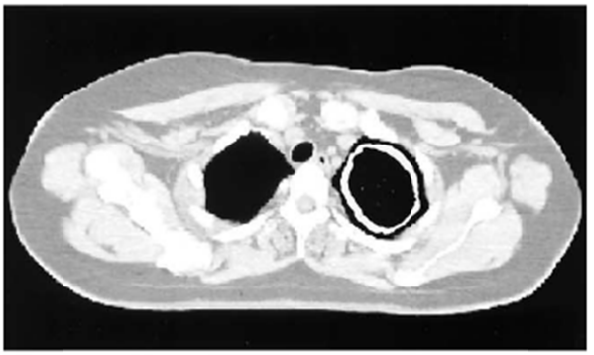

(B)

(C)

Figure 9. *(A–C) Evaluation of radiologic changes performed in the central and apical slice. In the central slice, three regions were analyzed.*

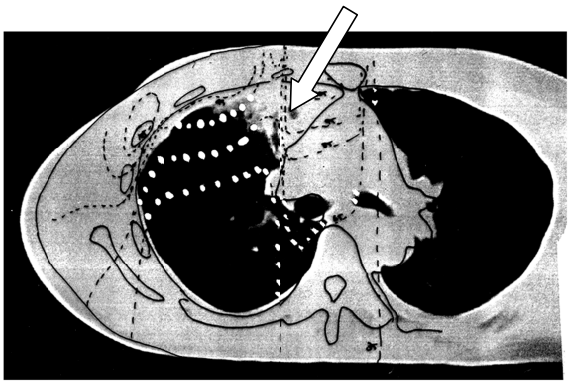

Figure 10 *Diagnostic CT scan of a lung reaction at arrow showing density changes, from low density (black) to high density (white) for treatment technique IV. Dose distribution schematically shown.*

Of the 121 patients included in this study, 24 were referred for local-postoperative RT and 97 for loco-regional therapy following either radical mastectomy (69) or partial mastectomy (28).
The patients were treated with four different RT techniques:

I. Local RT after partial mastectomy: tangential photons covering the breast to a total dose of 50 Gy at 2 Gy per fraction, 5 fractions a week.
II. Loco-regional RT after partial mastectomy including internal mammary lymph nodes (IMN): photons covering the breast and the fossa supraclavicular, axillar and IMN. Totaldose 50 Gy at 2 Gy/fraction, 5 fractions a week.
III. Loco-regional RT after partial mastectomy excluding internal mammary lymph nodes: as group II but excluding IMN. Totaldose 50 Gy at 2 Gy/fraction, 5 fractions a week.
IV. Loco-regional RT after modified radical mastectomy: the internal mammary, axillary, and supraclavicular lymph nodes were treated with photon beams and the chest wall with enface electrons. Total dose of 46 Gy at 2 Gy per fraction, 5 fractions a week.

The span in relative lung volumes irradiated with the four treatment techniques is illustrated for a subgroup in Figure 11 and shows the mean cumulative ipsilateral lung DVH for the four different RT techniques. The figure illustrates the relatively large span in doses to the lung for the different techniques. However, individual variations within each group (not illustrated here) were also significant. DVH was calculated using the Theraplan system, version 5B for both papers I and II. This system uses a pencil beam-like algorithm (the Batho-power law algorithm) to correct for inhomogeneities. The dose planning was based on about 20 CT slices with 1 cm spacing over the chest. Photon energies ranged from 4 MV up to 8 MV and electron energies from 6 MeV up to 16 MeV.

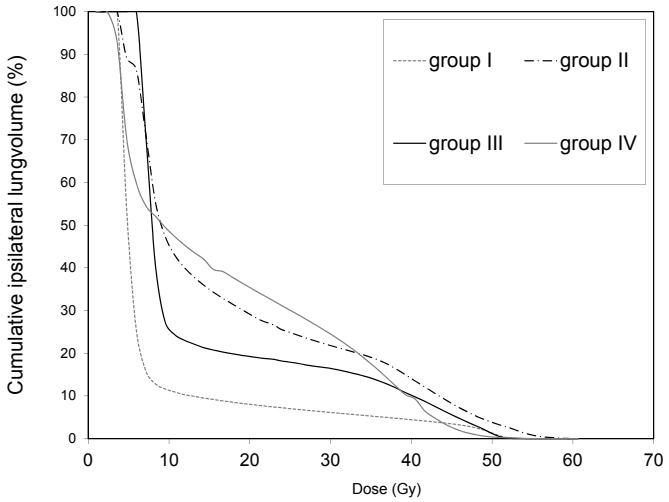

Figure 11. *Cumulative DVH of the ipsilateral lung volume showing the different subgroups in study I.*

Data on potentially confounding factors were also collected prior to RT. A clinical assessment for RP was done 1, 4, and 7 months after RT completion. RP was clinically defined according to the following criteria:

0. No RP: no registered respiratory symptoms or respiratory problems independent of RT, as judged by the clinician.
1. Mild RP: respiratory symptoms (cough and/or dyspnea with or without fever) judged by the clinician to be RT induced but not treated with corticosteroids.
2. Moderate complications: respiratory symptoms (cough and/or dyspnea with or without fever) judged by the clinician to be RT induced and requiring corticosteroid treatment.

The definition of mild and moderate reactions was similar to the NCI-CTC[32]. The patients were assessed by a few clinicians working closely together in a single centre to reduce the effect of different observer judgements in clinical findings. 28 patients (23%) developed symptomatic RP. In 23 patients (19%), mild RP was diagnosed, and in 5 patients (4%) moderate RP was diagnosed. If chemotherapy had been given, the therapy was finished 3 to 8 weeks before the start of RT.
The result of the study showed that short-term lung density changes and symptomatic RP were associated with:

- RT techniques
- Total doses as low as 16–30 Gy
- Increased age

No association was found between lung density changes and the following confounding factors were shown:

- Chemotherapy
- Concurrent tamoxifen intake
- Smoking habits

In paper II, a cohort of 87 of the above 121 patients were further analyzed. Correlations between the incidence of short-term pulmonary complications and lung-dose/volume and fractionation parameters were documented. Data from dose–volume histograms of the complete ipsilateral lung and incidence data were fitted with four different NTCP models. Each bin of the dose-volume histograms was corrected for fractionation to 2 Gy per fraction using the LQ model with a α/β ratio of 3 Gy. The end-points considered in this study were: symptomatic (clinical) RP, X-ray assessed lung density changes and CT assessed lung density changes.

Clinical pneumonitis was defined according to modified CTC-NCIC grades 0–2. Patients with of grade-1 or -2 pneumonitis were grouped together in the analysis and compared with asymptomatic patients. Density changes on chest X-ray were scored according to a system originally suggested by Arriagada[76] which divides the lung field into three regions: the apical-lateral, central-parahilar and basal-lateral. The highest density grades in each region were added together to form scores ranging from 0 to 9. Total scores of 1–3 were considered to represent slight radiological pneumonitis and scores of 4–9 moderate to severe.

Density changes on chest CT were evaluated using two scan sets of the thorax: the first one was taken prior to RT for treatment planning purposes and the second 4 months after the completion of RT. Each lung was divided into three regions and density changes were scored and grouped together in the same way as described above for the evaluation of chest X-ray changes. Also in this analysis no/slight RP was compared to moderate/ severe events.

The four different NTCP models used were: the Lyman model with DVH reduced to the equivalent uniform dose (LEUD), the Logit model with DVH reduced to EUD (LOGEUD), the Mean Lung Dose (MLD) model and the Relative Seriality (RS) model. The data-fitting procedure was done using the maximum likelihood analysis, based on individual DVHs and binary incidence data (0 = no complication, 1 = complication).

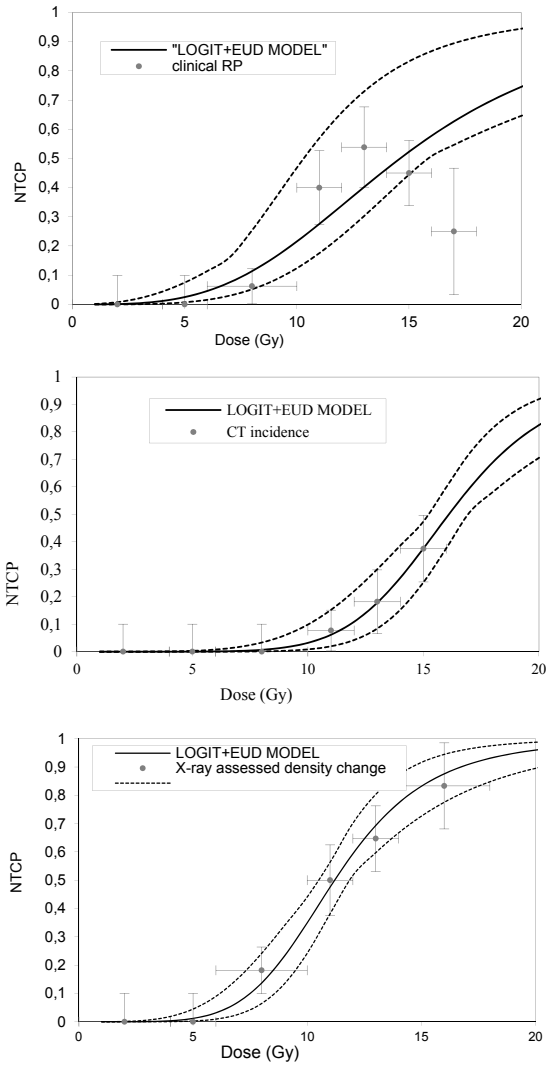

Figure 12. *Results for modelling with the LOGIT+EUD model. NTCP versus EUD is shown. The end-points were clinical RP (upper panel), incidence diagnosed by CT (middle panel) and X-ray assessed density changes (lower panel).*

Figure 12 shows the results of modelling for the *LOGIT+EUD* model. The incidence data in the figure (solid symbols) have been pooled and sorted into bins of 2 or 4 Gy. The solid line shows the results of modelling and the dotted lines the two-dimensional 68% confidence interval for the NTCP curve. All the studied NTCP models fit quite accurately the endpoints considered. EUD or MLD were shown to be robust and simple parameters correlated with the risk of RP. This result is consistent with those from other studies in which MLD correlated with the incidence of RP, although there is a large range of dose used for different studies[30].

The present study resulted in a D_{50} value significantly lower than many other studies, which might be explained by differences in the definition of the end-point. In this study only early pulmonary complications were evaluated.

In a continued work to reduce RP in BC patients treated with loco-regional RT at Södersjukhuset, the use of dose-volume constraints significantly reduced post-RT radiological changes on chest X-ray[77]. Symptomatic pneumonitis was very rare in this study. Only one patient of 88 developed a moderate reaction. Mild reactions were detected in 6 patients. Furthermore, no relationship was found between symptomatic RP and radiological RP on chest X-ray or CT, but only one patient was diagnosed with RP, so no statistically relevant conclusion can be made.

6.2 SBRT WITH HYPOFRACTIONATION (PAPERS III, IV, V)

SBRT with hypofractionation of tumors in the lungs differs considerably from conventional RT for breast cancer with regards to both spatial and temporal dose distributions in the lungs, as described above. Although these two treatment methods represent extremes, investigations of both provides considerable insight into the radio response of lung tissue. In SBRT the questions to be analyzed are similar to those for BC when modelling complications, but an additional important question in SBRT is the analysis of uncertainties in dose due to the algorithm for dose computation in dose planning and of breathing motions during the treatment[78].

In paper III the accuracy of the calculated spatial dose distribution in SBRT for tumors in the lungs, including breathing motions were investigated. The accuracy of a number of dose planning algorithms in commercial systems (Eclipse, TMS-HELAX and Pinnacle) were investigated by comparison with Monte-Carlo (MC) calculated dose distributions in a phantom for two different tumors, diameters of 2 and 5 cm, located in lung equivalent material. The geometry of the phantom was cylindrical with a pentagonal cross section and with the tumor in the center, surrounded by lung. The geometries were simple enough to be accurately implemented in the MC code and in the TPSs but still amenable to study uncertainties stemming both from algorithms and motions. Five beams of 6 MV, were used to represent typical SBRT dose plans. Dose calculations were done with two simple pencil beam algorithms and two superposition-convolution algorithms in which the change in lateral transport of secondary particles in lung is accounted for. The impact of breathing motions on dose to target and to lung was also investigated by using MC simulations. In these, published patient data for breathing motion patterns were used including both longitudinal and transverse motions but simplified to a linear motion without the hysteresis seen in actual patient data[79, 80]. Longitudinal and lateral dose distributions were calculated as well as dose-volume histograms for target volumes, lung minus GTV and PTV minus GTV.

The analysis showed that the dose in the central part of the gross tumor volume (GTV) is calculated for both tumor sizes with an accuracy of 2–3% with pencil

beam and superposition-convolution algorithms, compared to MC calculation, as shown in Figure 13 below.

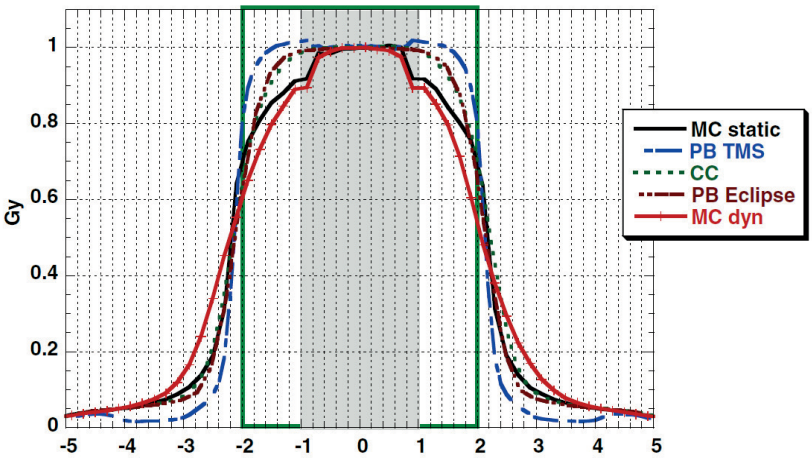

Figure 13. *Simulated dynamic case. Calculated longitudinal dose profiles for a simulated 2 cm tumor in lung tissue. Pencil beam algorithms, TMS and Eclipse, as well a superposition-convolution algorithm (CC) is compared to MC for both static and a dynamic case with a respiratory motion up to ±16 mm. Gray area represents the GTV and green square PTV.*

At the periphery of the GTV, the dose planning algorithms overestimate the dose up to 10%, whereas in the lung tissue between PTV and GTV pencil beam algorithms generally overestimate the dose and the superposition-convolution underestimates it. Furthermore, there are differences between the two pencil beam algorithms as well as between the two superposition-convolution algorithms.

Two different respiratory motion patterns, representing different amplitudes, were included in the dose calculation with the MC. From the results of these calculations it was concluded that the dose to the GTV was considered relatively accurately estimated by the dose planning algorithms and the MC simulations for the static situation, as shown in Figure 13. On the other hand, the dose at the periphery of the GTV is overestimated, compared to the static case. A "narrowing" of the longitudinal dose profile of up to 20 mm (at about 90% dose level) is seen relative the static dose profile calculated with the pencil beam algorithms. An explanation for the relatively small impact on the dose to GTV, when breathing motions are included, is the inhomogeneous dose distribution in the PTV. The GTV is moving into higher and lower dose regions with the respiratory motion, which are partly compensating for each other.

An important conclusion from this investigation is that failure to consider breathing motions in the dose calculation will have a smaller impact than the choice of dose planning algorithm when one estimates the dose that will actually be delivered. This result is, however, based on the use of a very inhomogeneous dose distribution within the PTV and cannot be applied for a homogeneous dose

distribution as used in conventional RT. Furthermore, the algorithm used must be reported together with dosimetric data in publications on follow-up data.

In paper IV, the impact of fractionation correction with the LQ and USC models was investigated for the modelling of lung toxicity after SBRT for lung tumors. The toxicity data used were from 57 patients included in a phase II multicenter trial on SBRT for medically inoperable stage I NSCLC; of this group 10.5% were diagnosed with RP2+[42]. The prescribed dose to target was 22 Gy x 3 at the isocenter with 15 Gy per fraction at the periphery of the PTV. The dose planning involved two simple pencil beam algorithms implemented in two different TPSs, TMS-Helax and Eclipse. The dose to the high dose regions, in the volume between PTV and CTV was overestimated according to results in paper III and the dose to the lung volume outside the PTV was underestimated (Figure 13). Attempts were made to find a simplified dose correction algorithm to correct for the lack of accuracy of pencil beam algorithms to be applied on DVH data retrospectively. Because these attempts were unsuccessful, original dose data were used in the NTCP modelling. To investigate the impact of fractionation correction two different models the LQ model[81] and the USC model[53, 54] were applied to dose data for each individual DVH for lung minus GTV. The NTCP-modelling was done using the Lyman-Kutcher-Burman (LKB) model[63, 65].

Parameter values of D_0 and $\bar{n}$ in the USC model were determined from estimated values of α and d_T. In the LQ model a α/β ratio of 3 Gy was used. In the fitting procedure, parameter values of n in the LKB model were determined for a range of values of m and D_{50}, so the mean NTCP for the 57 patients was 10.5%, in accordance with the incidence.
The result of the NTCP modelling indicates a more serial like response of the lung with the USC correction for fractionation, as compared to that with LQ correction. As a consequence, low dose volumes were found to contribute less and high dose volumes more to the NTCP when using the USC model compared to the LQ model. Still, additional clinical data are needed in order to reach more reliable conclusions.

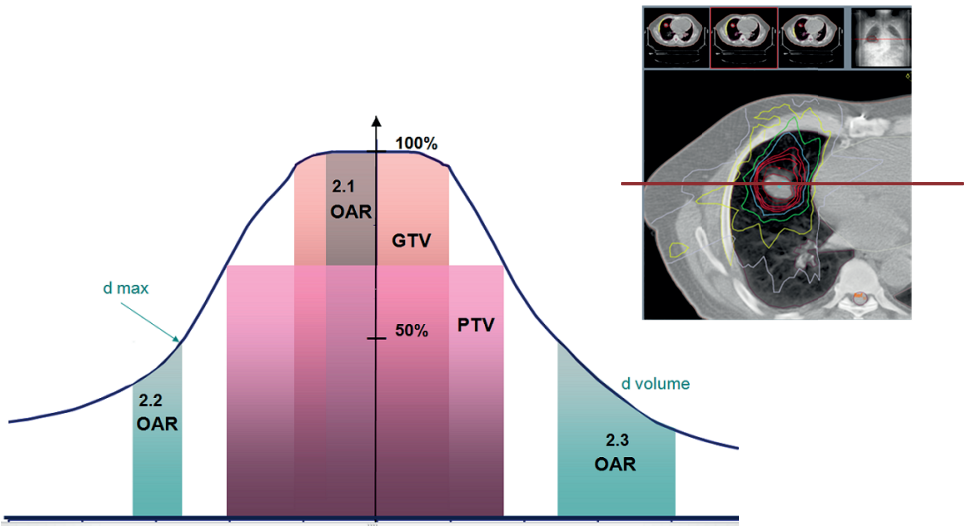

Figure 14. *Doseprofile through lung and tumor for a typical SBRT treatment. GTV, PTV and OAR are shown. Inserted shows dose distribution from the SBRT technique showing the central plane.*

The consequences of the results from paper IV was further investigated in paper V, in which the impact on the therapeutic window were evaluated using the two different models, USC and LQ, for fractionation correction in a range of regimes with 2 to 20 fractions at target doses common in SBRT. Three different scenarios were studied as illustrated in Figure 14.
First, the OAR receives a homogeneous dose equal to the dose to the GTV (denoted 2.1). Isoeffective doses (constant cell survival) for tumor and normal tissue were calculated with the two models, with 22 Gy x 3 as a reference. Second, the OAR receives a fraction of the prescribed dose, and the response is assumed to be proportional to maximum dose (denoted 2.2). Cell survival was calculated at the point of maximum dose, with the two models, for isoeffective tumor doses, also here with 22 Gy x 3 as a reference. Third, the OAR receives a fraction of the prescribed dose and the response is assumed to be proportional to the complete dose distribution in the OAR (denoted 2.3). Normal tissue complication probability (NTCP) was calculated, with correction for fractionation with the two models, for iso-effective tumor doses using parameters obtained in paper IV. Three different reference situations were investigated with 15 Gy x 3, 22 Gy x 3 and 29.3 Gy x 3.

In the all three scenarios (2.1-2.3) the tumor was assumed to have a fractionation sensitivity corresponding to α/β equal to 10 Gy in the LQ model and parameter values of the USC model, according that of NSCLC as used in paper IV. The OAR was assumed to have parameter values as determined for the lung in paper IV and with a α/β ratio equal to 3 Gy for the LQ model.

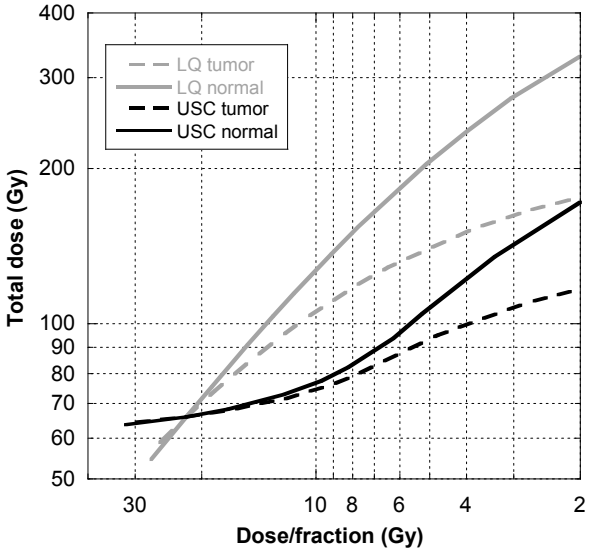

Figure 15 *Calculated isoeffect curves, normalized to 22 Gy x 3 for tumor and normal tissues using LQ or USC for fractionation correction. The number of fraction increases to the right on the dose/fraction axis.*

At a dose per fraction below about 6 Gy (case 2.1) the LQ and USC models predict the same fractionation sensitivity (slope) as shown in Figure 15. At a high dose per fraction, above about 15 Gy, the USC model predicts much lower fractionation sensitivity, compared to the LQ model. Further the therapeutic window was shown to increase with an increasing number of fractions in SBRT, compared to the commonly used three fractions. Both the LQ and USC models predicted this outcome, but generally a clearly greater gain is predicted with the USC model. Specifically, the USC model predicts a higher sensitivity for fractionation than the LQ model (for iso effective tumor doses) if the OAR receives less than the dose given to the GTV. The greater gain predicted by the USC model applied to both cases, denoted as 2.2 and 2.3 in Figure 15.

The results from paper V have had an impact on clinical SBRT at Karolinska University Hospital in the sense that large tumors and centrally located lung tumors with adjacent sensitive structures are generally treated now with 8 to 10 fractions. Furthermore, a phase II multicenter trial on patients with lung tumors located less than 1 cm from the main/lobar bronchi has been initiated from Karolinska. Here, 8 fractions with 7 Gy/fraction are given at the periphery of the PTV. Other centres have also adopted a less extreme hypo fractionation than 3 for lung tumors at a central location. At VUMC in Amsterdam 8 x 7.5 Gy have been used and preliminary results on local control are similar to those from treating with 5 x 12 Gy or 3 x 20 Gy, with generally very low toxicity[82]. This preliminary clinical result indicates very low fractionation sensitivity at very high doses/fraction in correspondence to the results in Figure 12.

7 CONCLUSION AND FUTURE POSSIBILITIES

In this thesis radiation induced side effects in lung tissue after radiotherapy in the thorax region were studied. The overall aim was to investigate how radiation induced side-effects correlates with and can be modelled in terms of the spatial and temporal distributions of the dose delivery in conventional RT for BC and hypofractionated SBRT for lung cancer.
The results showed, first, that short-term lung density changes and symptomatic RP were associated with RT techniques after RT for BC. The apical part of the lung appeared to be less radiation sensitive than the central part. Furthermore, RP grade I after RT for BC was accurately modelled with NTCP models and EUD and MLD are simple parameters that correlate with the risk of RP.

Second, for SBRT of lung tumors, the accuracy in dose to the GTV is relatively insensitive with respect to the algorithm used for dose planning, even considering breathing motions at dose delivery. However, at the periphery of the GTV and especially in the lung tissue outside but close to the GTV, the dose is considerably overestimated with the simplest algorithms. Improved algorithms that take into account the change in lateral transport of secondary particles is, however, relatively accurate in the estimation of dose to the lung.
From incidence data of RP grade 2 or more after SBRT of lung tumors, parameter values in the LKB NTCP model were determined for the lung using both the LQ and USC models for fractionation correction. The parameter values so determined were used to investigate the impact on the therapeutic window with increasing numbers of fractions in SBRT for lung tumors. When fractionation correction with the LQ and USC models were compared a larger gain was predicted by the USC model by increasing the number of fractions from 3 to about 10. At a very high dose per fraction the sensitivity for fractionation is considerably lower as predicted by the USC model compared to that for the LQ model.

To use dose/volume constraints that are available in the literature, knowledge of underlying data is important. Uncertainties in clinical response data stem partly from the difficulty of specifying end-points that are straightforward to quantify. For the lungs, the response to radiation is to some extent a continuous effect with a gradual change in severity. In general, there is a lack of accurate data for the more severe end-points.
To safely use dose/volume constraints today only the context in which they were created may be relevant. However, this would restrict the use of dose-response relations in the generation of hypotheses for developments in RT. Thus, consistent modelling of dose/volume parameters in the determination of dose-response relations will be more fruitful for the future.
The causes of some uncertainties in dose delivery to the patients are set-up errors and organ motions, which can make the delivered dose unreliable compared to the calculated dose to an organ. Uncertainties in *static* dose calculations are today a minor problem because relatively accurate dose planning algorithms based on Monte Carlo simulations are now available, as are the superposition-convolution algorithms now in use. Still, dose calculation that takes into account organ motion

and deformations must be implemented if uncertainties in calculated dose to OAR are to be reduced. Uncertainties in dose-response relations are highly dependent of how the correction for fractionation is done in the data gathered, especially for high doses per fraction.

To assure the reliable prediction of side-effects, more clinical studies are needed and the uncertainties in both the definition of clinical findings and in dose delivery have to be addressed and reduced.

8 ACKNOWLEDGEMENTS

Some of these studies were supported by grants. I wish to thank The Swedish Cancer Society, the King Gustaf Vth Jubilee Fund, the Alex and Eva Wallström Society and the Swedish Medical Society.

I would like to express my sincere gratitude to all those who directly or indirectly contributed to the completion of this work.

Special thanks to the Medical Physics department, Karolinska Sjukhuset who have supported this work through all the years.

To members of the study groups – both at Södersjukhuset (lung toxicity in BC) and the Nordic SBRT study group.

To my patient and understanding supervisor Ingmar Lax for all the invaluable advice.

To my late mentor, Lennart Sundbom, who initiated my interest for research– I am sure that he is still watching over me.

To all my friends and colleagues who have listened to my thoughts and encouraged me to continue. No one is forgotten.

Extra thanks to my supportive friends Giovanna, Bruno, Åsa, Younes, Massoud, Pierre, Mathias, Eija, Ann-Sofi and Ing-Marie. Without you nothing would have been possible.

And also to Anna and the Aria-group – keeping me sane.

To my fellow PhD students Vanessa, Pia and Ulla. We are soon all of us PhDs. Hooray!!

To all my friends and relatives – it is never too late …..

And finally to my family Emilia, Alex och Lars, who have waited for me to come home a million times. A zillion hugs and kisses for all the missed ones.

Berit

9 REFERENCES

1. P. Mayles, A. Nahum and Rosenwald, "Handbook of Radiotherapy Physics: Theory and Practice," edited by T. Francis (2007).
2. D. Hanahan and R. A. Weinberg, "The Hallmarks of Cancer," Cell **100**, 57-70 (2000).
3. International Commission On Radiation Units And Measurement, "Prescribing, Recording and Reporting Photon Beam Therapy (ICRU)," *Vol. 50,* (1993).
4. H. Thames and J. Hendry, *Fractionation in radiotherapy*. (Taylor and Francis, London, 1987).
5. S. A. Bapat, "Evolution of cancer stem cells," Seminars in Cancer Biology **17**, 204-213 (2007).
6. H. Withers, "Cell cycle redistribution as a factor in multifraction irradiation.," Radiology **114**, 199-202 (1975).
7. H. R. Withers, "Lethal and sublethal cellular injury in multifraction irradiation," European Journal of Cancer (1965) **11**, 581-583 (1975).
8. H. P. Rodemann and M. A. Blaese, "Responses of Normal Cells to Ionizing Radiation," Seminars in Radiation Oncology **17**, 81-88 (2007).
9. M. Joiner and A. van der Kogel, "Basic Clinical Radiobiology ", (Hodder Arnold, 2009).
10. E. B. Podgorsak, "Radiation Oncology Physics: A Handbook for Teachers and Students," in *Educational Report Series,* (IAEA, Vienna, 2005).
11. Socialstyrelsen, "Cancer Incidence in Sweden 2009," in *Sveriges officiella statistik, Hälso och Sjukvård,* (2010).
12. M. Overgaard, P. S. Hansen, J. Overgaard, C. Rose, M. Andersson, F. Bach, M. Kjaer, C. C. Gadeberg, H. T. Mouridsen, M.-B. Jensen and K. Zedeler, "Postoperative radiotherapy in high-risk premenopausal women with breast cancer who receive adjuvant chemotherapy.," N Engl J Med **337**, 949-955 (1997).
13. M. Overgaard, M. B. Jensen, J. Overgaard, P. S. Hansen, C. Rose, M. Andersson, C. Kamby, M. Kjaer, C. C. Gadeberg, B. B. Rasmussen, M. Blichert-Toft and H. T. Mouridsen, "Postoperative radiotherapy in high-risk postmenopausal breast-cancer patients given adjuvant tamoxifen: Danish Breast Cancer Cooperative Group DBCG 82c randomised trial [see comments]," Lancet **353**, 1641-1648 (1999).
14. J. Ragaz, S. M. Jackson, N. Le, I. H. Plenderleith, J. J. Spinelli, V. E. Basco, K. S. Wilson, M. A. Knowling, C. M. L. Coppin, M. Paradis, A. J. Coldman and I. A. Olivotto, "Adjuvant radiotherapy and chemotherapy in node-positive premenopausal women with breast cancer," N Engl J Med **337**, 956-962 (1997).
15. P. McGale, S. C. Darby, P. Hall, J. Adolfsson, N.-O. Bengtsson, A. M. Bennet, T. Fornander, B. Gigante, M.-B. Jensen, R. Peto, K. Rahimi, C. W. Taylor and M. Ewertz, "Incidence of heart disease in 35,000 women treated with radiotherapy for breast cancer in Denmark and Sweden," Radiotherapy and Oncology **100**, 167-175 (2011).
16. N. Martini, M. S. Bains, M. E. Burt, M. F. Zakowski, P. McCormack, V. W. Rusch and R. J. Ginsberg, "Incidence of local recurrence and second primary tumors in resected stage I lung cancer," The Journal of Thoracic and Cardiovascular Surgery **109**, 120-129 (1995).
17. X. Qiao, O. Tullgren, I. Lax, F. Sirzen and R. Lewensohn, "The role of radiotherapy in treatment of stage I non-small cell lung cancer," Lung Cancer **41**, 1-11 (2003).
18. G. S. Sibley, "Radiotherapy for patients with medically inoperable Stage I nonsmall cell lung carcinoma: smaller volumes and higher doses - a review.," Cancer **82**, 433-438 (1998).
19. M. Werner-Wasik, E. Yorke, J. Deasy, J. Nam and L. B. Marks, "Radiation Dose-Volume Effects in the Esophagus," International Journal of Radiation Oncology*Biology*Physics **76**, S86-S93 (2010).
20. International Commission On Radiation Units And Measurement, "Prescribing, Recording and Reporting Photon Beam Therapy," *Vol. 50,* (1993).
21. S. M. Bentzen, L. S. Constine, J. O. Deasy, A. Eisbruch, A. Jackson, L. B. Marks, R. T. Haken and E. D. Yorke, "Quantitative Analyses of Normal Tissue Effects in the Clinic (QUANTEC)," Int J Radiat Oncol Biol Phys **76** (2010).

22. L. B. Marks, X. Yu, Z. Vujaskovic, W. Small, R. Folz and M. S. Anscher, "Radiation-induced lung injury," Seminars in Radiation Oncology **13**, 333-345 (2003).
23. S. Delanian and J.-L. Lefaix, "Current Management for Late Normal Tissue Injury: Radiation-Induced Fibrosis and Necrosis," Seminars in Radiation Oncology **17**, 99-107 (2007).
24. D. Stanley, "The uniform reporting of treatment-related morbidity," Seminars in Radiation Oncology **4**, 112-118 (1994).
25. P. Lind, G. Svane, G. Gagliardi and C. Svensson, "Abnormalities by pulmonary regions studied with computer tomography following local or local-regional radiotherapy for breast cancer," International Journal of Radiation Oncology*Biology*Physics **43**, 489-496 (1999).
26. M. Guckenberger, K. Heilman, J. Wulf, G. Mueller, G. Beckmann and M. Flentje, "Pulmonary injury and tumor response after stereotactic body radiotherapy (SBRT): Results of a serial follow-up CT study," Radiotherapy and Oncology **85**, 435-442 (2007).
27. P. Lind, H. Bylund, B. Wennberg, C. Svensson and G. Svane, "Abnormalities on chest radiographs following radiation therapy for breast cancer," European Radiol **10**, 484-489 (2000).
28. K. L. Stephans, T. Djemil, S. M. Gajdos, C. A. Reddy and G. M. M. Videtic, "Dosimetric Variables Predictive of Pulmonary Function Test (PFT) Changes After Stereotactic Body Radiotherapy (SBRT) for Stage I Lung Cancer," International Journal of Radiation Oncology*Biology*Physics **69**, S496-S497 (2007).
29. M. T. Milano, L. S. Constine and P. Okunieff, "Normal Tissue Tolerance Dose Metrics for Radiation Therapy of Major Organs," Seminars in Radiation Oncology **17**, 131-140 (2007).
30. L. B. Marks, S. M. Bentzen, J. O. Deasy, F.-M. Kong, J. D. Bradley, I. S. Vogelius, I. El Naqa, J. L. Hubbs, J. V. Lebesque, R. D. Timmerman, M. K. Martel and A. Jackson, "Radiation Dose–Volume Effects in the Lung," International Journal of Radiation Oncology*Biology*Physics **76**, S70-S76 (2010).
31. A. Jackson, L. B. Marks, S. M. Bentzen, A. Eisbruch, E. D. Yorke, R. K. Ten Haken, L. S. Constine and J. O. Deasy, "The Lessons of QUANTEC: Recommendations for Reporting and Gathering Data on Dose–Volume Dependencies of Treatment Outcome," International Journal of Radiation Oncology*Biology*Physics **76**, S155-S160 (2010).
32. National Cancer Institute, "Common Toxicity Criteria NCI-CTC v2," in *http://www.eortc.be/services/doc/ctc/ctcv20_4-30-992.pdf*, (1999).
33. Radiation Oncology Group and European Organization for Research and Treatment of Cancer, "RTOG/EORTC Acute and Late Radiation Morbidity Scoring schema," in *http://www.rtog.org/ResearchAssociates/AdverseEventReporting/RTOGEORTCLateRadiationMorbidityScoringSchema.aspx*
http://www.rtog.org/ResearchAssociates/AdverseEventReporting/AcuteRadiationMorbidityScoringCriteria.aspx.
34. S. L. Faria, M. Aslani, F. S. Tafazoli, L. Souhami and C. R. Freeman, "The Challenge of Scoring Radiation-induced Lung Toxicity," Clinical Oncology **21**, 371-375 (2009).
35. S. M. Bentzen, J. Z. Skoczylas, M. Overgaard and J. Overgaard, "Radiotherapy-related lung fibrosis enhanced by tamoxifen," J Natl Cancer Inst **88**, 918-922 (1996).
36. S. Johansson, L. Bjermer, L. Franzen and R. Henriksson, "Effects of ongoing smoking on the development of radiation-induced pneumonitis in breast cancer and oesophagus cancer patients [see comments]," Radiother Oncol **49**, 41-47 (1998).
37. P. Lind, B. Wennberg, G. Gagliardi and T. Fornander, "Pulmonary complications following different radiotherapy techniques for breast cancer, and the association to irradiated lung volume and dose," Breast Cancer Res Treat **68**, 199-210 (2001).
38. P. Lind, S. Rosfors, B. Wennberg, U. Glas, S. Bevegard and T. Fornander, "Pulmonary function following adjuvant chemotherapy and radiotherapy for breast cancer and the issue of three-dimensional treatment planning," Radiotherapy and Oncology **49**, 245-254 (1998).
39. I. Lax, H. Blomgren, I. Näslund and R. Svanström, "Stereotactic Radiotherapy of Malignancies in the Abdomen: Methodological aspects," Acta Oncologica **33**, 677-683 (1994).

40. H. Blomgren, I. Lax, I. Näslund and R. Svanström, "Stereotactic High Dose Fraction Radiation Therapy of Extracranial Tumors Using An Accelerator: Clinical experience of the first thirty-one patients," Acta Oncol. **34**, 861 - 870 (1995).
41. Z. Fuks and R. Kolesnick, "Engaging the vascular component of the tumor response," Cancer Cell **8**, 89-91 (2005).
42. P. Baumann, J. Nyman, M. Hoyer, B. Wennberg, G. Gagliardi, I. Lax, N. Drugge, L. Ekberg, S. Friesland, K. A. Johansson, J. A. Lund, E. Morhed, K. Nilsson, N. Levin, M. Paludan, C. Sederholm, A. Traberg, L. Wittgren and R. Lewensohn, "Outcome in a prospective phase II trial of medically inoperable stage I non-small-cell lung cancer patients treated with stereotactic body radiotherapy," J Clin Oncol **27**, 3290-3296 (2009).
43. B. D. Kavanagh and R. Timmerman, "Stereotactic Body Radiotherapy," edited by W. W. Lippincott (2005).
44. B. D. Kavanagh, R. C. McGarry and R. D. Timmerman, "Extracranial Radiosurgery (Stereotactic Body Radiation Therapy) for Oligometastases," Seminars in Radiation Oncology **16**, 77-84 (2006).
45. R. D. Timmerman, K. M. Forster and L. Chinsoo Cho, "Extracranial Stereotactic Radiation Delivery," Seminars in Radiation Oncology **15**, 202-207 (2005).
46. M. Hoyer, H. Roed, A. T. Hansen, L. Ohlhuis, J. Petersen, H. Nellemann, A. K. Berthelsen, C. Grau, S. A. Engelholm and H. von der Maase, "Prospective study on stereotactic radiotherapy of limited-stage non-small-cell lung cancer," International Journal of Radiation Oncology*Biology*Physics **66**, S128-S135 (2006).
47. P. Baumann, J. Nyman, M. Hoyer, G. Gagliardi, I. Lax, B. Wennberg, N. Drugge, L. Ekberg , S. Friesland, K.-A. Johansson, J.-Å. Lund, E. Morhed, K. Nilsson, N. Levin, M. Paludan, C. Sederholm, A. Traberg, L. Wittgren and R. Lewensohn, "Stereotactic Body Radiotherapy for medically inoperable patients with stage I non-small cell lung cancer- a first report of toxicity related to COPD/CVD in a prospective phase II study " Radiother Oncol **88**, 359-367 (2008).
48. Y. Seppenwoolde, K. De Jaeger, L. J. Boersma, J. S. A. Belderbos and J. V. Lebesque, "Regional differences in lung radiosensitivity after radiotherapy for non-small-cell lung cancer," International Journal of Radiation Oncology*Biology*Physics **60**, 748-758 (2004).
49. T. T. Puck and P. I. Markus, "Action of X-rays on mammalian cells.," Journal of Experimental Medicin **103**, 653-666 (1976).
50. M. M. Elkind and G. F. Whitmore, "The radiobiology of cultured mammalian cells," edited by G. Breach (New York 1967).
51. J. F. Fowler, R. H. Thomlinson and A. E. Howes, "Time-dose relationships in radiotherapy," European Journal of Cancer (1965) **6**, 207-221 (1970).
52. H. D. Thames Jr, R. Withers, K. A. Mason and B. O. Reid, "Dose-survival characteristics of mouse jejunal crypt cells," International Journal of Radiation Oncology*Biology*Physics **7**, 1591-1597 (1981).
53. J. P. Kirkpatrick, J. J. Meyer and L. B. Marks, "The Linear-Quadratic Model Is Inappropriate to Model High Dose per Fraction Effects in Radiosurgery," Seminars in Radiation Oncology **18**, 240-243 (2008).
54. C. Park, L. Papiez, S. Zhang, M. Story and R. D. Timmerman, "Universal Survival Curve and Single Fraction Equivalent Dose: Useful Tools in Understanding Potency of Ablative Radiotherapy," International Journal of Radiation Oncology*Biology*Physics **70**, 847-852 (2008).
55. F. W. McKenna and S. Ahmad, "Fitting techniques of cell survival curves in high-dose region for use in stereotactic body radiation therapy," Physics in Medicine and Biology **54**, 1593 (2009).
56. J. F. Fowler, "Linear Quadratics Is Alive and Well: In Regard to Park et al. (Int J Radiat Oncol Biol Phys 2008;70:847-852)," International Journal of Radiation Oncology*Biology*Physics **72**, 957-957 (2008).
57. A. M. Chen, D. G. Farwell, Q. Luu, L. M. Chen, S. Vijayakumar and J. A. Purdy, "Marginal Misses After Postoperative Intensity-Modulated Radiotherapy for Head and Neck Cancer," International Journal of Radiation Oncology*Biology*Physics **80**, 1423-1429 (2011).
58. L. B. Marks, E. D. Yorke, A. Jackson, R. K. Ten Haken, L. S. Constine, A. Eisbruch, S. M. Bentzen, J. Nam and J. O. Deasy, "Use of Normal Tissue Complication Probability

Models in the Clinic," International Journal of Radiation Oncology*Biology*Physics **76**, S10-S19 (2010).
59. E. D. Yorke, "Modeling the effects of inhomogeneous dose distributions in normal tissues," Seminars in Radiation Oncology **11**, 197-209 (2001).
60. Y. Seppenwoolde and J. V. Lebesque, "Partial irradiation of the lung," Seminars in Radiation Oncology **11**, 247-258 (2001).
61. P. Källman, PhD thesis, Stockholm University, 1992.
62. J. V. Lebesque, Y. Seppenwoolde, J. S. Belderbos, K. de Jaeger, G. T. Henning, J. A. Hayman, M. K. Martel and R. K. Ten Haken, "Radiation pneumonitis and NTCP models," International Journal of Radiation Oncology*Biology*Physics **51**, 86-87 (2001).
63. J. T. Lyman, "Complication probability as assessed from dose-volume histograms," Radiat Res Suppl **8**, S13-S19 (1985).
64. G. J. K. a. C. Burman, "Calculation of complication probability factors for non-uniform normal tissue irradiation: The effective volume method," Int J Radiat Oncol Biol Phys **16**, 1623-1630 (1989).
65. G. J. Kutcher and C. Burman, "Calculation of complication probability factors for non-uniform normal tissue irradiation: The effective volume method," Int J Radiat Oncol Biol Phys **16**, 1623-1630 (1989).
66. S. L. S. Kwa, J. C. M. Theuws, A. Wagenaar, E. M. F. Damen, L. J. Boersma, P. Baas, S. H. Muller and J. V. Lebesque, "Evaluation of two dose-volume histogram reduction models for the prediction of radiation pneumonitis," Radiotherapy and Oncology **48**, 61-69 (1998).
67. S. L. S. Kwa, J. V. Lebesque, J. C. M. Theuws, L. B. Marks, M. T. Munley, G. Bentel, D. Oetzel, U. Spahn, M. V. Graham, R. E. Drzymala, J. A. Purdy, A. S. Lichter, M. K. Martel and R. K. Ten Haken, "Radiation pneumonitis as a function of mean lung dose: an analysis of pooled data of 540 patients," International Journal of Radiation Oncology*Biology*Physics **42**, 1-9 (1998).
68. D. A. Jaffray, P. E. Lindsay, K. K. Brock, J. O. Deasy and W. A. Tomé, "Accurate Accumulation of Dose for Improved Understanding of Radiation Effects in Normal Tissue," International Journal of Radiation Oncology*Biology*Physics **76**, S135-S139 (2010).
69. M. van Herk, D. Jaffray, A. Betgen, P. Remeijer, J. Sonke, M. Smitsmans, L. Zijp and J. Lebesque, "First clinical experience with cone-beam CT guided radiation therapy; evaluation of dose and geometric accuracy," International Journal of Radiation Oncology*Biology*Physics **60**, S196 (2004).
70. J. A. Purdy, "Photon dose calculations for three-dimensional radiation treatment planning," Seminars in Radiation Oncology **2**, 235-245 (1992).
71. M. Engelsman, E. M. F. Damen, P. W. Koken, A. A. van 't Veld, K. M. van Ingen and B. J. Mijnheer, "Impact of simple tissue inhomogeneity correction algorithms on conformal radiotherapy of lung tumours," Radiotherapy and Oncology **60**, 299-309 (2001).
72. K. De Jaeger, M. S. Hoogeman, M. Engelsman, Y. Seppenwoolde, E. M. F. Damen, B. J. Mijnheer, L. J. Boersma and J. V. Lebesque, "Incorporating an improved dose-calculation algorithm in conformal radiotherapy of lung cancer: re-evaluation of dose in normal lung tissue," Radiotherapy and Oncology **69**, 1-10 (2003).
73. V. Panettieri, B. Wennberg, G. Gagliardi, M. Duch, M. Ginjaume and I. Lax, "SBRT of lung tumours: Monte Carlo simulation with PENELOPE of dose distributions including respiratory motion and comparison with different treatment planning systems," Phys Med Biol. **52**, 4265-4281 (2007).
74. J. O. Deasy, S. M. Bentzen, A. Jackson, R. K. Ten Haken, E. D. Yorke, L. S. Constine, A. Sharma and L. B. Marks, "Improving Normal Tissue Complication Probability Models: The Need to Adopt a "Data-Pooling" Culture," International Journal of Radiation Oncology*Biology*Physics **76**, S151-S154 (2010).
75. P. Lind, Doctoral thesis, Karolinska Institute, 1999.
76. R. Arriagada, J. Laudron de Guevara and H. Mouriesse, "Limited small cell lung cancer treated by combined radiotherapy and chemotherapy: evaluation of a grading system of lung
fibrosis.," Radiother Oncol **14**, 1-8. (1989).

77. U. Blom-Goldman, B. Wennberg, G. Svane, H. Bylund and P. Lind, "Reduction of radiation pneumonitis by V20-constraints in breast cancer.," Radiation Oncology **5** (2010).
78. I. Lax, V. Panettieri, B. Wennberg, M. A. Duch, I. Näslund, P. Baumann and G. Gagliardi, "Dose distributions in SBRT of lung tumors: Comparison between two different treatment planning algorithms and Monte-Carlo simulation including breathing motions," Acta Oncol. **45**, 978 - 988 (2006).
79. Y. Seppenwoolde, H. Shirato, K. Kitamura, S. Shimizu, M. van Herk, J. V. Lebesque and K. Miyasaka, "Precise and real-time measurement of 3D tumor motion in lung due to breathing and heartbeat, measured during radiotherapy," International Journal of Radiation Oncology*Biology*Physics **53**, 822-834 (2002).
80. G. S. Mageras and E. Yorke, "Deep inspiration breath hold and respiratory gating strategies for reducing organ motion in radiation treatment," Seminars in Radiation Oncology **14**, 65-75 (2004).
81. D. J. Brenner, "The Linear-Quadratic Model Is an Appropriate Methodology for Determining Isoeffective Doses at Large Doses Per Fraction," Seminars in Radiation Oncology **18**, 234-239 (2008).
82. M. Dahele, J. R. van Sörnsen de Koste, B. Slotman and S. Senan, "Adaptive Strategies to Reduce Toxicity of Stereotactic Body Radiotherapy (SBRT) for Large Stage I Lung Tumors," International Journal of Radiation Oncology*Biology*Physics **78**, S527 (2010).